

# Chemostratigraphy of the Upper Carboniferous Schooner Formation, southern North Sea

T. J. Pearce,<sup>1</sup> D. Wray,<sup>2</sup> K. Ratcliffe,<sup>1</sup> D. K. Wright,<sup>1</sup> A. Moscariello<sup>3</sup>

1. Chemostrat Ltd, Units 3–4, Llanfyllin Enterprise Park, Llanfyllin, Powys, SY22 5DD (office@chemostrata.co.uk)

2. Department of Earth Sciences, University of Greenwich, Chatham Maritime, Kent, ME4 4TB

3. Research & Technical Services, Shell International Exploration & Production, Volmerlaan 8, PO Box 60, 2289 AB Rijswijk, The Netherlands

## Summary

The virtually barren, mainly redbed sequences of the Schooner Formation (Upper Carboniferous) of the southern North Sea are an important gas reservoir, although well placement and reservoir development are hampered by the lack of a reliable stratigraphical framework. Chemostratigraphy has enabled the Schooner Formation encountered in well 44/21-3 to be divided into three chemostratigraphical units (S1, S2 and S3) and eleven sub-units (S1a–f, S2a–b and S3a–c), based on variations in mudstone and sandstone geochemical data acquired from core samples and cuttings. The geochemical characteristics of the units can be related to variations in mineralogy, depositional environment, climate and provenance. The units are correlated sub-regionally and the correlation is used to corroborate seismic correlations. A high-resolution chemostratigraphical zonation and correlation based on sub-units redefines models of reservoir architecture and enhances reservoir development in the nearby Schooner field.

Traditionally, interwell correlation for most reservoir sequences is achieved by using a combination of seismic, wireline log, biostratigraphical and sedimentological data. However, these techniques cannot always produce the required resolution for detailed stratigraphical modelling, particularly when dealing with barren fluvial sequences. Furthermore, the occurrence of thick monotonous successions of sandstones and mudstones, with repetitive wireline log characteristics and no prominent seismic reflectors, often makes correlating such sequences difficult. To refine the stratigraphy of such successions, palaeomagnetism (Hauger et al. 1994), heavy-mineral analysis (Morton 1985, 1991, Morton & Hallsworth 1994, Mange-Rajetzky 1995, Morton & Hurst 1995) and isotopic techniques (Mearns 1988, 1989) are often utilized, although their success is often hampered by poor sample quality, insufficient sample volume, or dependency upon a specific lithology. Consequently, a method is needed that can generate independent stratigraphical frameworks for barren well sections (and fossiliferous successions) and is not restricted by sample type. Such a method is chemical stratigraphy, or as it is more commonly known, chemostratigraphy.

This paper presents the results of a chemostratigraphical investigation on the virtually barren continental mudstones and sandstones that make up the Upper Carboniferous Schooner Formation (or “Barren Red Measures”) from the Silver Pit Basin, southern North Sea. These deposits form an ideal subject on which to test chemostratigraphy, as the sandstones represent significant gas plays, but their interwell correlation has proved notoriously difficult. Geochemical data are acquired from the mudstones and sandstones, and those data related to detrital minerals are used to erect a correlative chemostratigraphical zonation for the Schooner Formation. Furthermore, integration of these data with sedimentological information shows how the depositional environments, weathering styles and pedogenic

processes have affected sediment geochemistry. Pearce et al. (2005) incorporated the data presented herein into a multidisciplinary study utilizing palynology, clay-mineral data, heavy-mineral data and Sm–Nd isotope data to produce a new stratigraphical zonation and provenance model for the Schooner Formation.

## 1. Chemostratigraphy and correlation

For some time, bulk inorganic geochemical data have been used in correlating sequences (Pettijohn 1975), although the relatively recent advent of more efficient analytical techniques has resulted in more accurate data of this type being obtained. These techniques are inductively coupled plasma-optical emission spectrometry (ICP–OES) and inductively coupled plasma mass spectrometry (ICP–MS): they enable data to be acquired for the major elements and many trace elements. Chemostratigraphy has been applied to barren continental sequences (Ehrenberg & Siring 1992, Racey et al. 1995, Preston et al. 1998, Pearce et al. 1999, Ratcliffe et al. in press), although thick, rapidly deposited deltaic and marine sequences with poor biostratigraphical resolution also prove to be good subjects for chemostratigraphical studies (Pearce 1991, Pearce & Jarvis 1992a,b, 1995). Andrew et al. (1996) used chemostratigraphy in the Surat and Bowen basins in Australia to distinguish between Triassic Rewan and Showground formations for the purposes of petroleum exploration in sequences where conventional techniques such as lithostratigraphical, wireline and biostratigraphical analysis failed. Chemostratigraphy has also been applied to the correlation of tuffs in the Permian Newcastle and Wollombi Coal Measures in New South Wales in order to refine existing lithostratigraphical correlations (Kramer et al. 2001).

## 2. Study sequence

### 2.1 Geological setting and lithostratigraphy

In the southern North Sea, the successions lying beneath the Permian have been drilled in search of hydrocarbons with reservoir targets mostly within the Upper Carboniferous Coneybear Group (Cameron 1993). The sandy coal-measure deposits of the Langsettian and early Duckmantian are restricted to the northern part of the southern North Sea and are termed the Caister Coal Formation. They are overlain by argillaceous coal measures of the Westoe Coal Formation. At the end of Duckmantian times and during the early Bolsovian, grey sandy coal measures were again deposited in the Silver Pit area, followed by red silty mudstones and sandstones of later Bolsovian age. These deposits are all known as the Schooner Formation.

Significant erosion associated with the Saalian unconformity at the base of the Permian has, in places, removed part or all of the Schooner Formation, resulting in Permian successions directly sitting on either the Caister or Westoe coal formations. However, relatively thick redbed sequences are preserved in the axial regions of mainly northwest-southeast trending Variscan synclines in the Silver Pit area to the north of the Sole Pit inversion, although such sequences are either thin or absent over the crests of the complementary anticlines (Leeder & Hardman 1990, Cameron et al. 1992, Cameron 1993, Bailey et al. 1993).

### 2.2 Study wells

The study centres on well 44/21-3 (Fig. 1), as it has encountered one of the thickest Schooner Formation intervals and is a reference section for the formation (Cameron 1993; see Fig. 2). To

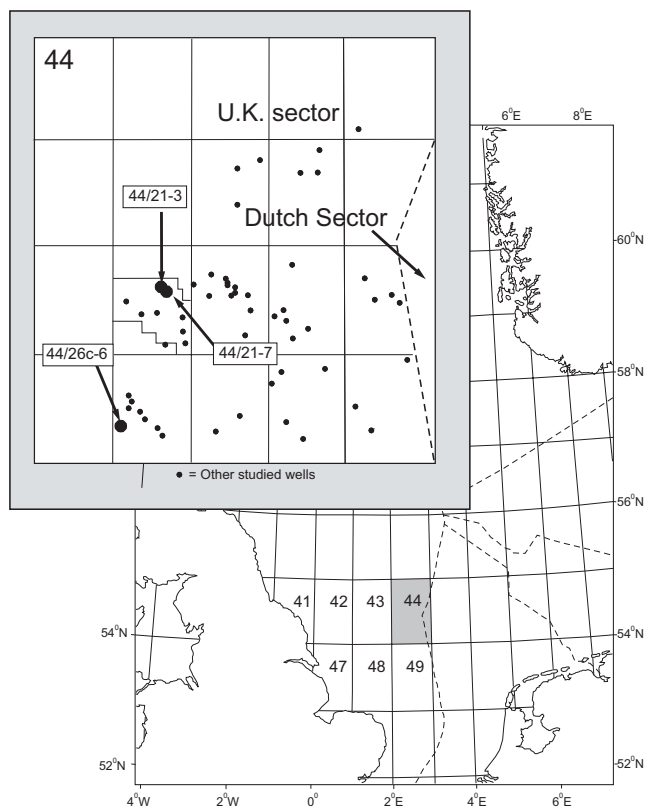


**Figure 1** Location of wells 44/21-3, 44/21-7 and 44/26c-6. The asterisk (\*) indicates the location of other UK sector wells that have penetrated the Schooner Formation and which have been the subjects of proprietary chemostratigraphical studies.

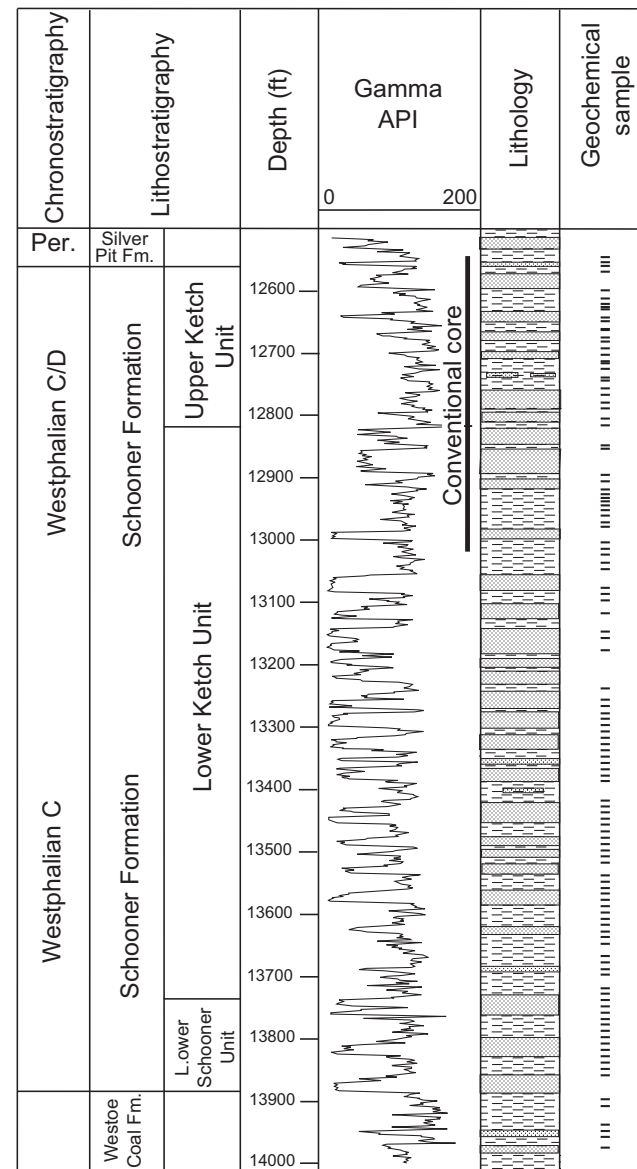


**Figure 2** Study interval of well 44/21-3. Lithostratigraphy from Cameron (1993).

test the correlation potential of chemostratigraphy, the Schooner Formation penetrated by well 44/26c-6 is also included in this study.

In well 44/21-3, the Schooner Formation is divided provisionally into the Lower Schooner Unit, which comprises grey sandy coal measures, and the Ketch Member (Fig. 2). This member consists of the Lower Ketch Unit, which corresponds to a relatively sandy redbed section, and the Upper Ketch Unit, an interbedded sequence of grey and red silty mudstones that also contains thin coals, caliches, limestones and sandstones (Fig. 2). Similar lithologies make up the Schooner Formation in well 44/26c-6, with the Lower Schooner Unit, and the Upper and Lower Ketch units, probably being present.

Above the formation are red mudstone beds of the Silverpit Formation (Fig. 2). A thin pebbly conglomerate marks the Saalian unconformity, which is put at 12 558 ft in well 44/21-3 (op. cit.). However, the base of the Schooner Formation is more difficult to recognize, because criteria such as the change from red to grey measures, or the first downhole occurrence of a thick coal seam, are used. The base of this formation is put at c. 13 884.3 ft

## CHEMOSTRATIGRAPHY OF THE UPPER CARBONIFEROUS SCHOONER FORMATION

in well 44/21-3 and corresponds to the base of the first thick clean sandstone encountered above the coal measures section.

### 3. Chemostratigraphy

#### 3.1 Methods

##### 3.1.1 Sampling rationale

At the start of a study, one needs to consider the scale of the intended chemostratigraphical correlation, the facies present over the study intervals and how closely spaced the samples should be.

If a detailed correlation of reservoir sections between closely spaced wells is the aim, then samples should be collected at 1–6 ft intervals, an objective best achieved over core sections. If, however, a broader, less detailed correlation is needed, then cuttings samples collected at 10–30 ft intervals should suffice. The fluvial sandbodies of the Schooner Formation probably have shoestring morphologies (Besly et al. 1993) and thus have very poor correlation potential, whereas the overbank mudstones have a much wider extent and consequently have a far better potential for correlation. Therefore, mudstone samples were collected in preference to sandstone samples from the Schooner Formation in well 44/21-3.

There is limited availability of core and sidewall core samples over the Schooner Formation of wells 44/21-3 and 44/21-7, which restricts the stratigraphical techniques that can be successfully applied to these sections. However, chemostratigraphy is not hampered by sample type. Only very small sample volumes are required for ICP analyses, and geochemical data of equally high quality and reliability can be acquired from cuttings and core samples (Jarvis & Jarvis 1992a,b, Pearce et al. 1999).

The grain size of sedimentary rocks has a significant impact on their geochemistry. Quartz (and thus  $\text{SiO}_2$ ), becomes increasingly abundant in coarser-grained sandstones, with the concentrations of the other elements subsequently decreasing, because of their dilution by quartz (Spears & Amin 1981, Shail & Floyd 1988). Consequently, coarse-grained and very coarse-grained sandstones are omitted from chemostratigraphical studies, as are breccias and conglomerates, because homogeneous samples cannot be reliably obtained from them. Suitable sandstone samples for ICP analysis can be difficult to acquire from cuttings, as during drilling these lithologies sometimes become disaggregated and thus are represented just by monomineralic grains. This can lead to possible grain-size and mineral fractionation.

Chips of mudstones and claystones are better preserved in the cuttings and tend to have uniform grain sizes. Therefore, any marked changes or trends recognized from the resultant geochemical datasets are likely to prove significant. Furthermore, these changes and trends probably will be fairly consistent over a wide area and so are very useful for correlation purposes (Cullers 1995). A relatively representative mudstone/claystone sample is obtained by picking about 200 chips of these lithologies from a cuttings sample. However, when only cuttings samples are available, the final resolution of the chemostratigraphical zonation and correlation will be controlled by the spacing of the analyzed samples; so, the greater the spacing, the less detailed will be the resolution. Moreover, only major long-term changes in sediment geochemistry can be recognized from datasets

derived just from cuttings (e.g. those related to changes in provenance or climate). Nevertheless, these changes probably will persist over an individual field or even subregionally, and will form the basis for any correlations.

Sandstone samples collected from core and sidewall cores are perfectly adequate for ICP-OES and ICP-MS analyses, but should be collected with reference to a sedimentological log if at all possible. Ideally, samples should be collected from the same facies and should be of similar grain size, thereby limiting any geochemical variations linked to these parameters. In practice, however, samples are taken from several broadly similar facies (very fine-grained to medium-grained sandstone), although poorly sorted sandstones are always excluded. Indurated sandstone chips can be collected from cuttings fairly easily, although usually more than 200 chips are picked from any one sample.

##### 3.1.2 Study material

The study interval in well 44/21-3 ranges from 12 560 ft to 14 000 ft, most of which covers the Schooner Formation and its subdivisions (Fig. 2). 117 mudstone samples and 15 sandstone samples have been analyzed by ICP-OES and ICP-MS techniques, with 44 samples coming from the core interval between 12 560 ft and 13 022 ft (= Upper Ketch Unit and the topmost part of the Lower Ketch Unit – Fig. 2). Sizes for the core samples are *c.* 1–2  $\text{cm}^3$  for the mudstones and *c.* 3–5  $\text{cm}^3$  for the sandstones. The remaining analyzed samples are cuttings from 13 025 ft–14 000 ft; a few of these come from the Westoe Coal Formation and only one comes from the Silverpit Formation (Fig. 2).

The sandstone geochemical dataset is relatively small and relates to a somewhat restricted stratigraphical interval. Consequently, geochemical data acquired from 49 Schooner Formation sandstone samples from nearby well 44/21-7 are incorporated into this dataset, so as to extend the stratigraphical range of the data (Fig. 1).

The well 44/26c-6 study interval is between 13 090 ft and 15 350 ft and extends from the base of the Silverpit Formation to cover the uppermost 600 ft of the Westoe Coal Formation. 56 mudstone samples collected from cuttings have been analyzed.

##### 3.1.3 Sample preparation and analysis

To avoid any contamination, all the samples are washed thoroughly prior to preparation for geochemical analysis; they are then ground in agate and dried. Subsamples weighing *c.* 0.25 g are prepared using a  $\text{LiBO}_2$  fusion (Jarvis & Jarvis 1992a,b). The resultant solutions are analyzed by ICP-OES and ICP-MS, with data being acquired for the major elements Si, Al, Ti, Fe, Mn, Mg, Ca, Na, K and P, the trace elements Ba, Co, Cr, Cs, Cu, Ga, Hf, Nb, Rb, Sc, Sr, Ta, U, V, Y, Zn and Zr, and the rare earth elements (REEs) La, Ce, Pr, Nd, Sm, Eu, Gd, Tb, Dy, Ho, Er, Yb and Lu (light rare earth elements LREEs = La–Nd, middle rare-earth elements MREEs = Sm–Ho and heavy rare-earth elements HREEs = Er–Lu). The analytical instruments are calibrated using certificated rock standards, with instrument drift being monitored after every five samples and, if necessary, corrected by the instrument software. The variability of data from multiple analyses of the reference rocks, and the comparison of these data with certified values, have enabled the precision and accuracy of the data to be assessed. Precision error is below 2 per cent for the major-element data and 3–6 per cent for the trace-element data and REE data.

### 3.2 Mudstone chemostratigraphy

One of the best ways to present the mudstone geochemical data is as geochemical profiles (Figs 3–5), which are constructed by plotting element concentrations against sample depth. In Figure 3, the  $Al_2O_3$  profile is based on absolute concentrations, whereas the other profiles and those in Figure 4 relate to  $Al_2O_3$ -normalized ratios for selected elements. Normalizing the data in this way nullifies any changes in geochemistry attributable to grain-size variations in the individual samples. The profile format enables element enrichments, depletions and significant stratigraphical geochemical trends to be recognized quite easily, from which a chemostratigraphical zonation can be developed. In addition, geochemical profiles based on other element ratios (e.g. Cr/Cs, Ta/U, etc.), are depicted in Figure 5 to highlight specific mineralogical trends.

The chemostratigraphical zonation of the Schooner Formation in well 44/21-3 is based on the data for the major elements  $Al_2O_3$ ,  $TiO_2$ ,  $Fe_2O_3$ ,  $MgO$ ,  $CaO$ ,  $K_2O$  and  $P_2O_5$ , the trace elements Cr, Cs, Hf, Nb, Ni, Rb, Ta, Th, Y and Zr, and the REES La and Ce, these elements being referred to as chemostratigraphical index elements.

Interpretation of the geochemical profiles for the index elements, most of which are illustrated in Figures 3–5, allows the well 44/21-3 study interval to be divided into units W, S1, S2, S3 and P. Their geochemical characteristics are described below. (Units and Sub-units may be referred to by their numbers alone hereinafter, e.g. Unit S1 as “S1” and Sub-unit S3a as “S3a”).

#### Unit W

- Low  $Fe_2O_3$  ratio values and relatively high  $MgO$  and  $Na_2O$  ratio values. Lower  $Fe_2O_3/MgO$ ,  $TiO_2/K_2O$ , Cr/Cs, Nb/Rb, Ta/U, but higher Cs/La ratios than S1 samples (Fig. 5).

#### Unit S1

- Lower overall  $K_2O$ , Rb, Mg and Th levels and higher Ti, Ta and LREE levels than the other units.
- Higher Ta/U values overall than units S2 and S3 (Fig. 5).
- Higher Ta/U,  $Fe_2O_3/MgO$ , Cr/Cs and Nb/Rb values and much lower Cs/Zr and Cs/La values than S3 (Fig. 5).
- $Na_2O$ , Cr, Ni and Yb ratio values increase upwards over the unit, whereas  $K_2O$ , Rb and Cs ratio values decrease upwards.
- The top of the unit is defined by abrupt upward decreases in the  $TiO_2$ , Ta, Nb, Zr and Hf ratio values.

Unit S1 is divided into sub-units S1a to S1f, as follows:

- Sub-unit S1a has higher  $K_2O$ , Rb, Cs and Cr ratio values and slightly lower  $TiO_2$  ratio values than S1b. The top of the sub-unit is defined by upward decreases in the  $K_2O$ , Rb and Cs ratio values.
- Sub-unit S1b has lower  $K_2O$ , Rb and Cs ratio values than sub-units S1a, S1c and S1d, with its top being marked by sudden upward increases in the  $K_2O$ ,  $Na_2O$ ,  $MgO$ , Rb and Cs ratio values. Sub-units S1a and S1b have higher  $Fe_2O_3/MgO$ ,  $TiO_2/K_2O$ , Nb/Rb and Ta/U values, and lower Cs/La values than S1c.
- Sub-unit S1c is geochemically the most distinctive of the six sub-units, having high  $K_2O$ , Rb and Cs ratio values and low  $TiO_2$ , Nb, Ta and Y ratio values, as well as lower  $Fe_2O_3/MgO$ ,  $TiO_2/K_2O$ , Nb/Rb and Ta/U values, and much higher Cs/La

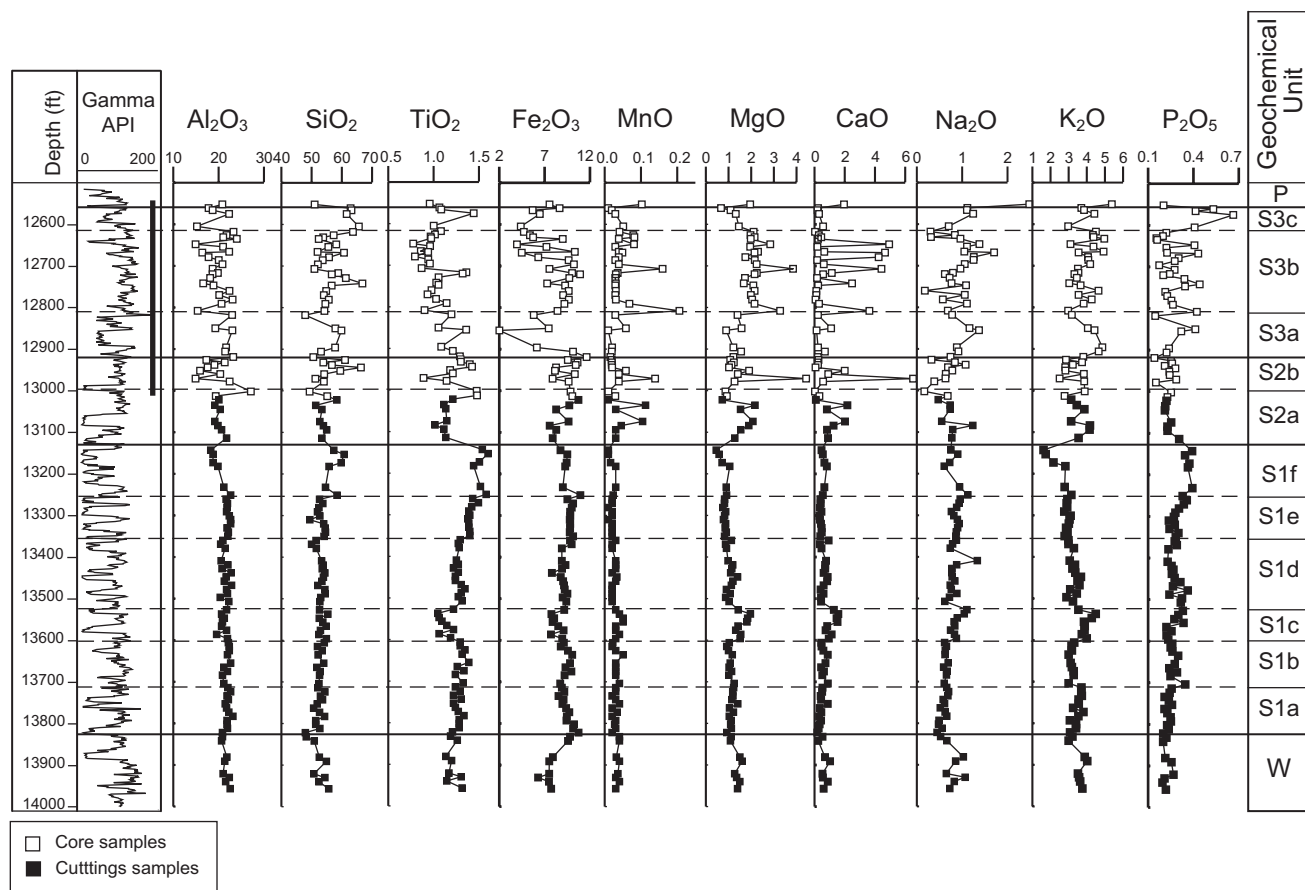


Figure 3 Major-element geochemical profiles: mudstone data. All values are weight per cent oxide.

CHEMOSTRATIGRAPHY OF THE UPPER CARBONIFEROUS SCHOONER FORMATION

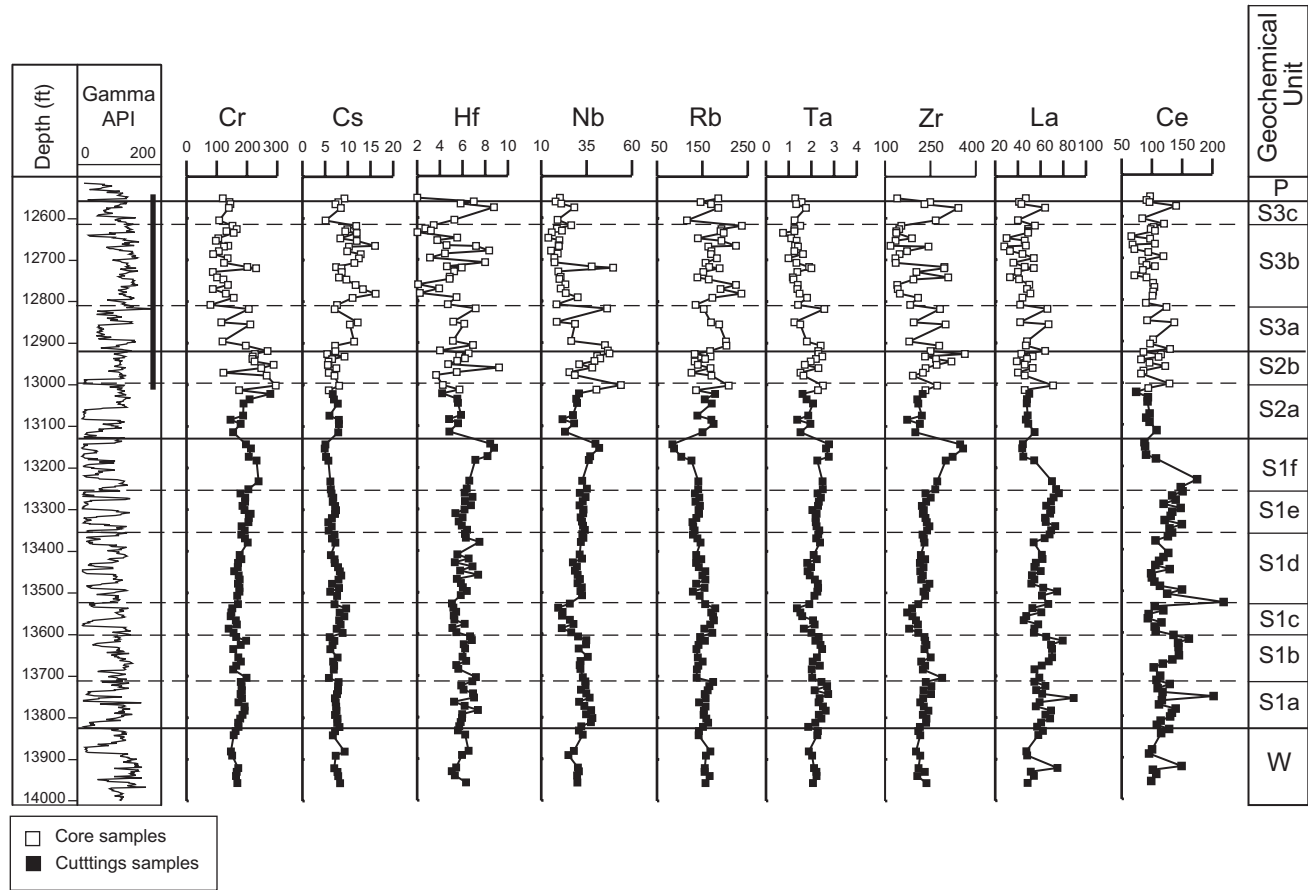


Figure 4 Selected trace-element geochemical profiles: mudstone data. All values are parts per million (ppm).

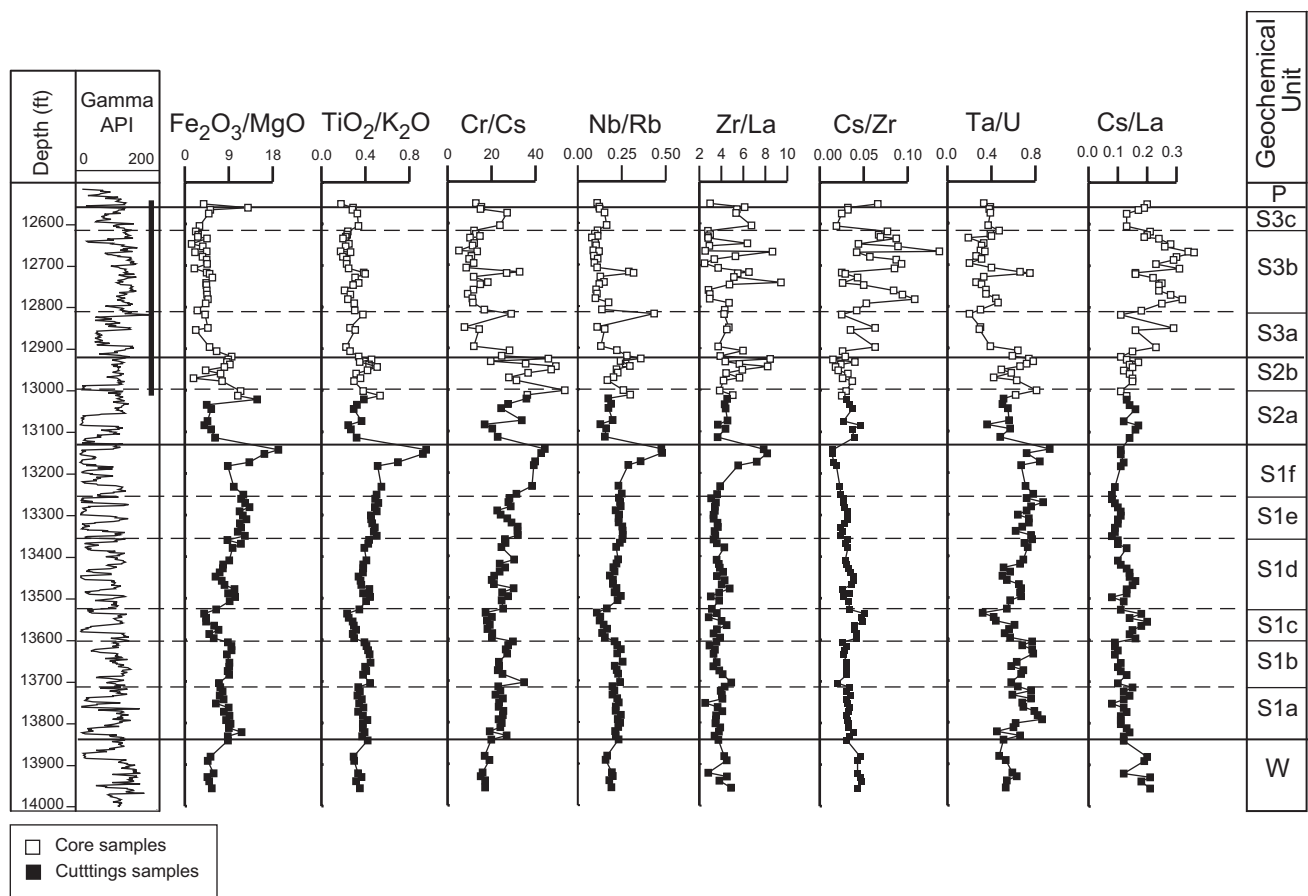


Figure 5 Geochemical profiles for selected element ratios: mudstone data.

values (Fig. 5). The corresponding interval also coincides with changes in the gradients of the  $\text{TiO}_2$ ,  $\text{Fe}_2\text{O}_3$ , Nb and Ta profiles. The top of the sub-unit is marked by abrupt upward decreases in the  $\text{K}_2\text{O}$ ,  $\text{Na}_2\text{O}$ , MgO, Rb and Cs ratio values, and sudden upward increases in the  $\text{TiO}_2$ , Nb and Ta ratio values.

- $\text{TiO}_2$ , Nb, Ta, Zr and Hf ratio values steadily increase upwards over the S1d–S1f interval, whereas  $\text{K}_2\text{O}$ , Rb and Cs ratio values decrease upwards (Figs 3, 4). Sub-unit S1d has lower  $\text{TiO}_2$ , Nb, Ta, Zr and Hf ratio values than the other two sub-units, as well as higher  $\text{K}_2\text{O}$ , Rb and Cs ratio values, with its top being defined by stepped upward decreases in the latter three ratio values (Figs 3, 4). The geochemical characteristics of S1e are transitional between those of sub-units S1d and S1f, although its top is marked by a sudden upward increase in the Cr ratio values (Fig. 4). Sub-unit S1f has higher  $\text{TiO}_2$ , Ta, Nb, Zr, Hf and Y ratio values than the other two sub-units and its  $\text{Fe}_2\text{O}_3/\text{MgO}$ ,  $\text{TiO}_2/\text{K}_2\text{O}$ , Nb/Rb and Zr/La values are the highest recorded from the study interval.

#### Unit S2

- Transitional geochemical characteristics between those of units S1 and S3, e.g.  $\text{K}_2\text{O}$ , MgO, Rb,  $\text{TiO}_2$  and Nb ratio values (Figs 3 and 4).
- Higher Cr ratio values than the other units.
- The unit top is defined by an abrupt upward increase in the Cs ratio values, less well defined increases in the  $\text{K}_2\text{O}$  and Rb ratio values, and sudden decreases in the Nb and Cr ratio values.
- Much higher  $\text{Fe}_2\text{O}_3/\text{MgO}$ ,  $\text{TiO}_2/\text{K}_2\text{O}$ , Nb/Rb and Ta/U values, and lower Cs/Zr and Cs/La values than S3 (Fig. 5).

Unit S2 is divided into sub-units S2a and S2b, as follows:

- Sub-unit S2a has lower Cr, Ni, Nb, Zr and Hf ratio values.
- Sr ratio values increase upwards over S2a, but then decrease upwards over S2b.
- Sub-unit S2b has significantly higher Cr/Cs and Zr/La values.

#### Unit S3

- The highest  $\text{K}_2\text{O}$ , Rb and Cs ratio values and the lowest  $\text{TiO}_2$ , Nb and Cr ratio values (Figs 3, 4).
- Localized very high CaO, MgO and MnO levels (Fig. 3).
- The highest Cs/Zr and Cs/La values, as well as low  $\text{Fe}_2\text{O}_3/\text{MgO}$ ,  $\text{TiO}_2/\text{K}_2\text{O}$ , Nb/Rb and Ta/U values (Fig. 5).

Unit S3 is divided into sub-units S3a, S3b and S3c, as follows:

- Sub-unit S3a has lower  $\text{Fe}_2\text{O}_3$  and MgO ratio values than sub-units S3b and S3c. Its top is marked by a coaly interval characterized by low Ta/U and Cs/La values.
- Sub-unit S3b has high MgO and  $\text{Fe}_2\text{O}_3$  ratio values, along with localized very high CaO levels. It also has the highest Cs/Zr and Cs/La values.
- $\text{TiO}_2$  and Nb ratio values generally decrease upwards over sub-units S3a and S3b, with the top of S3b being defined by the termination of these trends. These ratio values are higher in S3c.

#### Unit P

Only one analyzed sample (12552.5 ft) from the basal red mudstones of the Silverpit Formation is assigned to Unit P. The geochemical characteristics of the unit are similar to those of S3b and S3c, although it has much higher  $\text{Na}_2\text{O}$  and  $\text{K}_2\text{O}$  ratio values

(Fig. 3).

The above units and sub-units can be further characterized by using ternary diagrams. The sample plots define clusters on the ternary diagrams that can be related directly to the above units and sub-units (Fig. 6). For instance, units S1, S2 and S3 can be differentiated quite readily (Figs 6a–6c), as can most of the sub-units (Figs 6d–6i). However, although S1c and S1f can be differentiated, the only other distinction that can be made between the remaining four S1 sub-units is between S1a–S1b and S1d–S1e (Figs 6g–6i).

## 4. Mudstone geochemistry and mineralogy

Chemostratigraphy is based on the recognition of distinctive characteristics from the sedimentary geochemical datasets. The presence of these distinctive features, or “geochemical fingerprints”, allows sedimentary sequences to be divided into chemostratigraphical units, each unit having its unique fingerprint. However, a geochemical fingerprint usually comprises only the data for a limited number of elements (chemostratigraphical index elements). Moreover, the elements used as index elements may vary between different areas and stratigraphical intervals, because of differences in:

- *Detrital mineralogy and provenance composition*: the mineralogy and geochemical composition of different source areas can vary considerably, which therefore influences the geochemistry of the sediments derived from them.
- *Depositional environment and facies*: some elements may become concentrated in certain depositional environments and facies.
- *Diagenesis*: under different diagenetic regimes including weathering and pedogenesis, many elements may become remobilized, resulting in the detrital geochemical signatures of the sediments being either modified or obliterated.

As the chemostratigraphical zonation of the well 44/21-3 study interval is based on mudstone geochemistry, the following section naturally focuses on the mineral affinities of the elements found in the mudstones. Indeed, the determination of any relationships between element concentrations and mineral distributions, combined with the results of descriptive statistics and principal component analysis, enables those factors controlling element distributions over the study interval to be established.

### 4.1 Principal component analysis

Principal component analysis (PCA) is used to recognize element associations and to infer element–mineral affinities. PCA involves redrawing the axis system of the mudstone dataset for  $n$ -dimensional data (using UNISTAT for Windows), such that points lie as close as possible to the axes. The derived variables, termed principal components, can express a large proportion of the total variance of the dataset with a smaller number of variables. In this study, PCA can determine which elements have similar distributions and can then use these associations to highlight the characteristics of the dataset (Fig. 7). The various associations themselves can give some idea as to the factors controlling the abundance and distribution of the elements (e.g. mineralogy or grain size).

The main element associations recognized from Figure 7 are:

- $\text{K}_2\text{O}$ , Rb and Cs have affinities with illite/mica and chlorite.

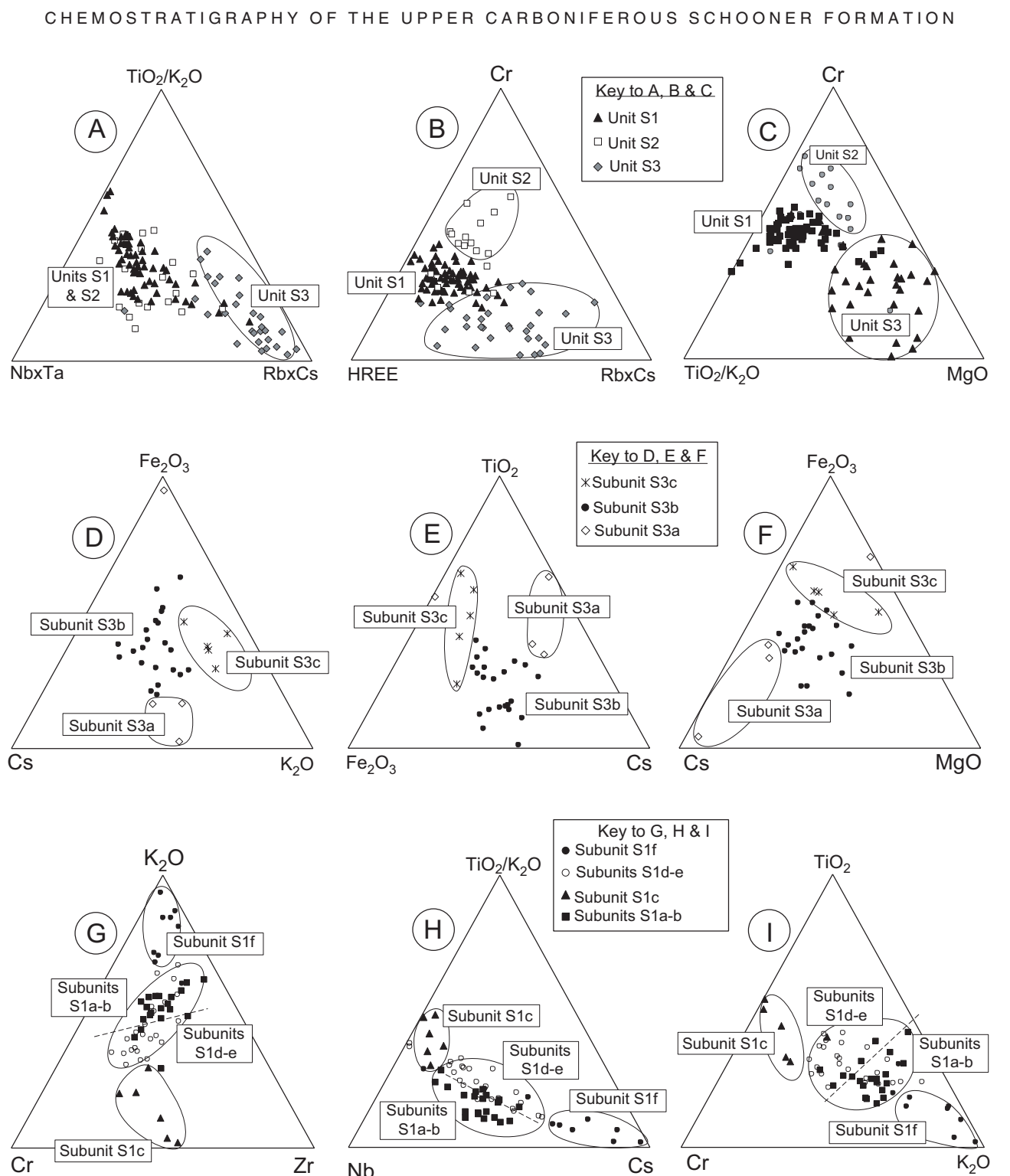


**Figure 6** Differentiation of mudstone samples using ternary diagrams. A–C plot data from S1, S2 and S3. D–F plot data for sub-units recognized in S3. G–I plot data for sub-units recognized in S1.

• CaO, MgO and MnO have affinities with carbonate minerals.

Al<sub>2</sub>O<sub>3</sub>, TiO<sub>2</sub>, Nb, Ta, Zr, Hf, Cr, the LREEs and the HREEs are all associated. Al<sub>2</sub>O<sub>3</sub> and the LREEs have affinities with the Al-oxyhydroxides and kaolinite, whereas Zr and Hf are linked with zircon. TiO<sub>2</sub>, Nb and Ta are connected with rutile and opaque minerals, although also have affinities with authigenic anatase and detrital clay. The HREEs are commonly concentrated in heavy minerals such as zircon, as well as clay minerals. Cr is associated with chrome-spinel, but is also relatively common in clay minerals and degraded mafic minerals.

The distribution of U, Co and Cu is primarily controlled by

the distribution of organic matter, higher values occurring in the grey mudstones. In contrast, these elements are depleted in the oxidized redbed intervals.

#### 4.2 Binary diagrams

The binary diagrams depicted in Figures 8 and 9 also highlight the element–mineral affinities, and Pearce et al. (2005) present clay-mineral and heavy-mineral data that corroborate the proposed affinities. Figure 8a shows that most of the mudstones have a relatively high SiO<sub>2</sub> content (about 60%), so silt-grade material (mostly as quartz grains) is probably fairly common.

T. J. PEARCE, D. WRAY, K. RATCLIFFE, D. K. WRIGHT, A. MOSCARIELLO

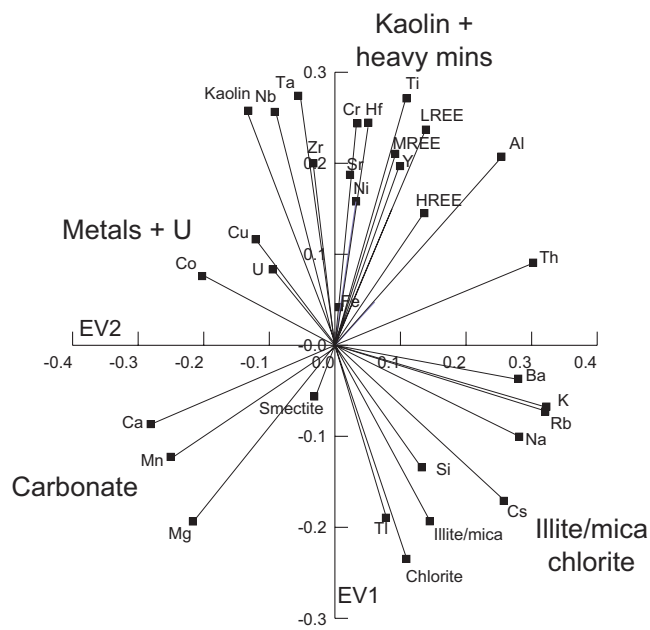


**Figure 7** Plots of eigenvector 1 (EV1) values versus eigenvector 2 (EV2) values. Four element associations are recognized: those associated with carbonate minerals, those linked with illite/mica and chlorite, those associated with kaolinite and heavy minerals, and those linked with metallic elements (see text for detailed discussions).

The abundances of  $K_2O$  and illite/mica are linked, with  $K_2O$  levels being relatively high in S1c. Illite/mica and smectite are the main clay minerals in S2 and S3a, although kaolinitic mudstone samples assigned to sub-units S2a and S3a have a relatively low  $K_2O$  content.  $Al_2O_3/K_2O$  values give some indication of the relative abundance of illite/mica and kaolinite, as  $K_2O$  is

abundant in illite/mica and  $Al_2O_3$  is abundant in kaolinite. Thus, increasing ratio values point to increasing kaolinite levels and vice versa, as exemplified by S1 and S3 (Fig. 8b), the latter unit having less kaolinite and more illite/mica than S1 (confirmed by Pearce et al. 2005). Furthermore, this demonstrates how  $K_2O$  and  $Al_2O_3$  data can provide some information about the stratigraphical distribution of these clay minerals.

Figure 7 shows Rb, Cs and  $Na_2O$  all have a close affinity with  $K_2O$ . Correlation coefficients for Rb: $K_2O$  (0.77) and for Rb:Cs (0.67; Fig. 8c) indicate that Rb and Cs levels are governed chiefly by variations in clay-mineral abundance. Apart from S3b, the plots of the S3 samples form a well defined linear trend on the Rb vs Cs binary diagram (Fig. 8d); the S3b samples do not plot on this trend, as they have high Cs levels. Cs levels increase at the base of S3b and coincide with the first appearance of chlorite (Pearce et al. 2005).

$Na_2O$  usually has affinities with clay minerals, feldspar and evaporite minerals. Halite and anhydrite cements occur locally in the sandstones near the top of the Ketch Member (Cameron 1993) and traces of anhydrite cement are recorded from the S3 sandstones in well 44/21-3 (Pearce et al. 2005). Nevertheless,  $Na_2O$  data from cuttings can be unreliable if drilling fluids have contaminated the samples. Moreover, most of the geochemical data included in this study come from cuttings, and whether or not drilling fluids have contaminated these samples is unknown, so the  $Na_2O$  data are ignored.

CaO and MgO are usually associated with calcite, dolomite and ferroan carbonates, with the relatively high CaO levels (5–6%) in S3 and S2b probably being related to dolomitized caliche horizons that formed during pedogenesis together with occasional freshwater limestones (Besly et al. 1993). High CaO and

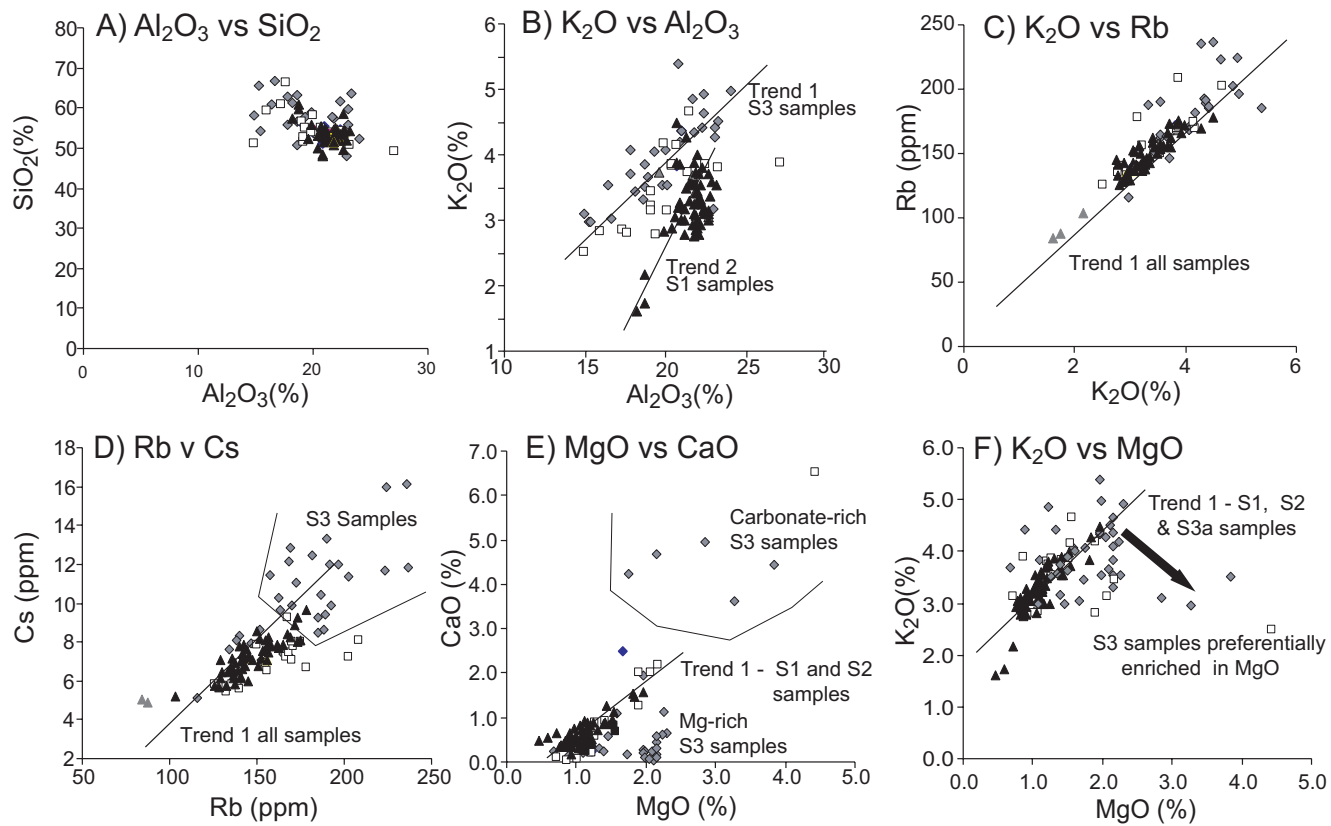


**Figure 8** Binary diagrams: mudstone data. The various illustrated diagrams allow S1, S2 and S3 to be differentiated.

## CHEMOSTRATIGRAPHY OF THE UPPER CARBONIFEROUS SCHOONER FORMATION

MgO levels together reflect the presence of carbonate minerals, whereas low concentrations are linked to clay minerals. These conclusions are supported by the positive linear trend defined by the S1 and S2 sample plots on Figure 8e. Only MgO levels are relatively high in S3, with sub-unit 3b having the highest levels of all (Fig. 8f); so here, MgO is probably associated with clay minerals, these high levels coinciding with an increase in chlorite (?corrensite)/smectite (Pearce et al. 2005).

Fe<sub>2</sub>O<sub>3</sub> concentrations are relatively high throughout the study interval, and in the red mudstones are associated with abundant disseminated haematite and other Fe-oxyhydroxides. In the red sandstones, haematite occurs as grain coats and pore fillings after siderite cements, as pseudomorphs after sphaerosiderite and as replacements of biotite, pyrite, clay matrix and sandstone clasts (Besly et al. 1993). However, localized siderite and ferroan dolomite cements are present in the mudstones, with caliche occurring in S3, all of which contribute to overall Fe<sub>2</sub>O<sub>3</sub> levels.

P<sub>2</sub>O<sub>5</sub> concentrations are relatively low in units S1 and S2,

although the higher P<sub>2</sub>O<sub>5</sub> levels in S3 most probably reflect the abundance of clay and organic matter in this unit. However, as apatite (a calcium phosphate) is present in the S3 sandstones (Pearce et al. 2005), so silt-grade apatite grains may occur in the mudstones, which thus may be the cause of the high P<sub>2</sub>O<sub>5</sub> levels in S3.

In sedimentary rocks, the REEs occur in feldspar, clay minerals, mica and heavy minerals, although their levels are very low in quartz. Consequently, REE concentrations are typically much higher in mudstones than sandstones. However, the mineral affinities of these elements in the well 44/21-3 samples are difficult to establish. LREE levels are highest in S1 and coincide with high Al<sub>2</sub>O<sub>3</sub> contents, which themselves are linked to the development of kaolinitic Al-oxyhydroxide soils. This element association is reflected by the overall positive relationship the LREE lanthanum (La) has with Al<sub>2</sub>O<sub>3</sub> (Fig. 9a) and its inverse relationship with K<sub>2</sub>O (Fig. 9b), which indicate that LREE levels are influenced by fractionation during pedogenesis and early diagenesis. LREE abundance may therefore be linked to clay

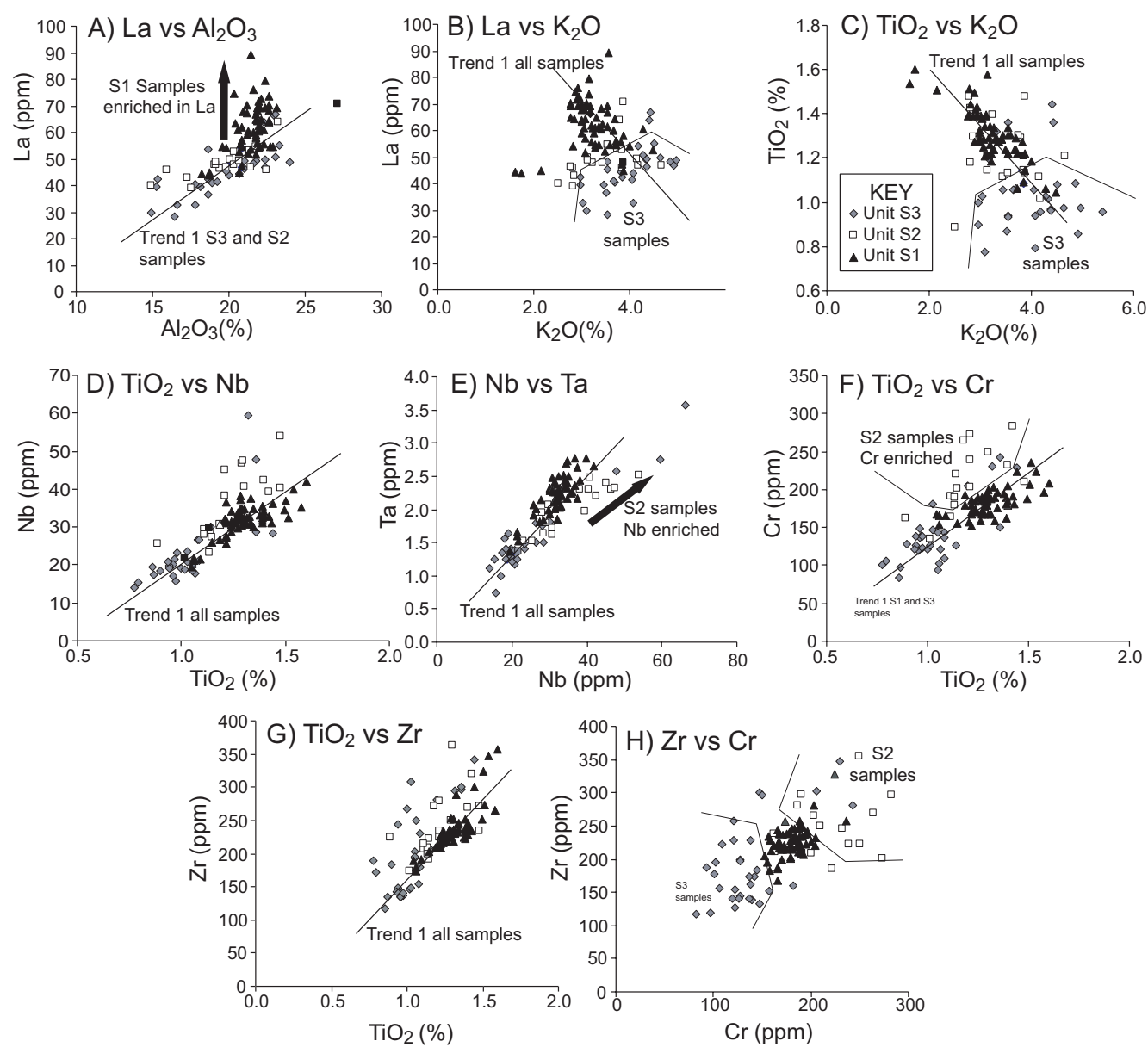


Figure 9 Binary diagrams: mudstone data. The various illustrated diagrams allow S1, S2 and S3 to be differentiated.

minerals and environmental conditions, because those elements tend to be more common in the oxidized kaolinitic S1 mudstones than in the S3 mudstones, which were deposited when the climate was more arid (Besly 2002).

TiO<sub>2</sub> concentrations are usually influenced by the occurrence of Ti oxides (rutile, ilmenite and anatase) and chlorite, illite/mica and biotite, although Figure 9c discounts any significant link between this element and illite/mica abundance. Instead, TiO<sub>2</sub> levels over the study interval are probably related to rutile (as silt- and sand-grade grains, as inclusions in detrital quartz grains (Blatt et al. 1972: 276, Scholle 1979: 9) and in lithic clasts), other Ti oxides such as anatase. Heavy-mineral data presented by Pearce et al. (2005) and Morton et al. (2005) confirm that rutile is a common detrital heavy-mineral phase in the Schooner Formation.

Figure 9d shows that Nb has a positive relationship with TiO<sub>2</sub> (Nb:TiO<sub>2</sub> correlation coefficient of 0.73), thus rutile abundance may well govern Nb levels. Ta also has a positive relationship with Nb (Fig. 9e) and, like Nb, Ta is associated with the distribution of rutile. Cr plots with a loose positive relationship (especially in samples from S1 and S3) with TiO<sub>2</sub> and with Zr (Fig. 9f-h), indicating that Cr is associated with the distribution of heavy minerals, particularly Cr-spinel, which is common in the Ketch Member (Morton et al. 2005).

Zr is linked to zircon, which is more common in S1 than in S3. The positive relationship between Hf and Zr (Zr:Hf correlation coefficient of 0.97) implies that Hf levels are controlled by zircon distribution and abundance.

### 5. Sandstone chemostratigraphy and mineralogy

The sandstone dataset for well 44/21-3 relates to the uppermost part of the Lower Ketch Unit and the Upper Ketch Unit. Added to the dataset are sandstone data acquired from the Lower Ketch Unit encountered in well 44/21-7. Although the well 44/21-3 dataset is too small to establish a chemostratigraphical zonation, the main geochemical characteristics of the sandstones can be summarized, certain element-mineral affinities can be established, and comments can be made regarding provenance.

The sandstone samples are classified by plotting some of their data on the "SandClass System" diagram devised by Herron (1988; see Fig. 10). This scheme enables the sandstones to be assigned to groups that are broadly equivalent to the categories defined by various mineralogical classification schemes (e.g. that of McBride 1963).

Most of the S3 sandstones are classified as litharenites, although the argillaceous ones plot in the Fe-shale, Fe-sand and wacke fields. Of the S2 sandstones, one is classified as a sublitharenite and the other two are Fe-sands. In contrast, the S1 sandstones of well 44/21-7 have higher SiO<sub>2</sub>/Al<sub>2</sub>O<sub>3</sub> values, which shows they are more quartzitic, and higher Fe<sub>2</sub>O<sub>3</sub>/K<sub>2</sub>O values, as they contain relatively abundant Fe oxyhydroxides, plus ferroan dolomite and ankerite cements. Consequently, most of them are classified as either quartz arenites or Fe-sands (Fig. 10) and are mineralogically more mature than the Upper Ketch sandstones.

Figures 11a-d show that the S1 sandstones can be differentiated from the S2 and S3 sandstones. The latter have more Al<sub>2</sub>O<sub>3</sub>

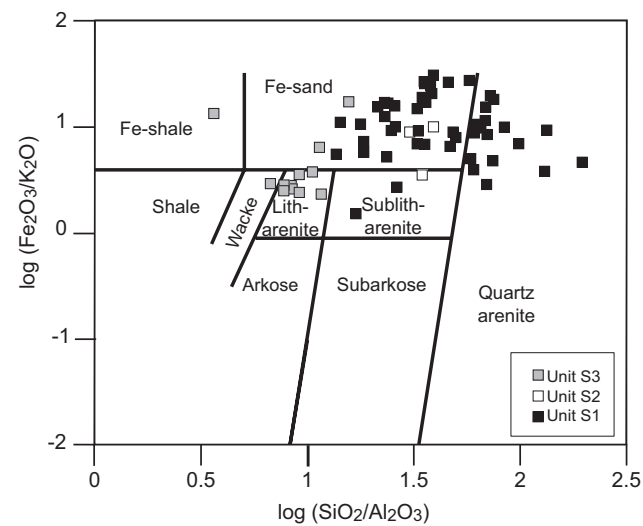


Figure 10 Geochemical classification of sandstones: wells 44/21-3 and 44/21-7. The sandstones are classified using the scheme of Herron (1988).

and K<sub>2</sub>O, the higher Al<sub>2</sub>O<sub>3</sub> levels reflecting their argillaceous nature, plus the presence of mica and, to a lesser extent, feldspar. Most of the sandstones have low CaO contents, although raised CaO levels in the S1 sandstones are attributed to ferroan dolomite cements, as Ca-bearing detrital minerals such as plagioclase feldspar are virtually absent. In the S2 and S3 sandstones, any high CaO levels are linked to dolomitic cements and, in some cases, the occurrence of rip-up caliche clasts.

The S1 sandstones from well 44/21-7 plot separately from the S2 and S3 sandstones of well 44/21-3 on Figure 11e. Zr levels are linked mainly with zircon, whereas Th can be associated with several minerals, including clay minerals and heavy minerals. Here, some of the Th is related to detrital clay, but most is linked to the relative abundance of zircon and apatite, thus as the S2 and S3 sandstones have more apatite, they therefore also have higher Th levels. The same sandstones also have more P<sub>2</sub>O<sub>5</sub> (Figs 11c,g), which again is partly associated with apatite.

Rb levels are typically higher in the S2 and S3 sandstones (Fig. 11f) as they have more detrital clay (illite/mica) and, to a lesser extent, more K feldspar. Detrital clay is virtually absent from the S1 sandstones, in which higher levels of La (an LREE) are associated with authigenic clay minerals, chiefly kaolinite.

The overall geochemical signature of the mudstones mimics that of the sandstones and demonstrates the mudstones are mineralogically mature, with relatively common silt-grade quartz and heavy-mineral grains.

### 6. Discussion

The following discussion presents a geological interpretation of the chemostratigraphical data. It also draws on the results of a mineralogical study outlined by Pearce et al. (2005).

#### 6.1 Sediment geochemistry, depositional environment and climate

When trying to recognize what impact, if any, climate change has had on the geochemistry of the Schooner Formation, there must first be some understanding of the regional climate during the time these sediments were deposited. The offshore Upper

CHEMOSTRATIGRAPHY OF THE UPPER CARBONIFEROUS SCHOONER FORMATION

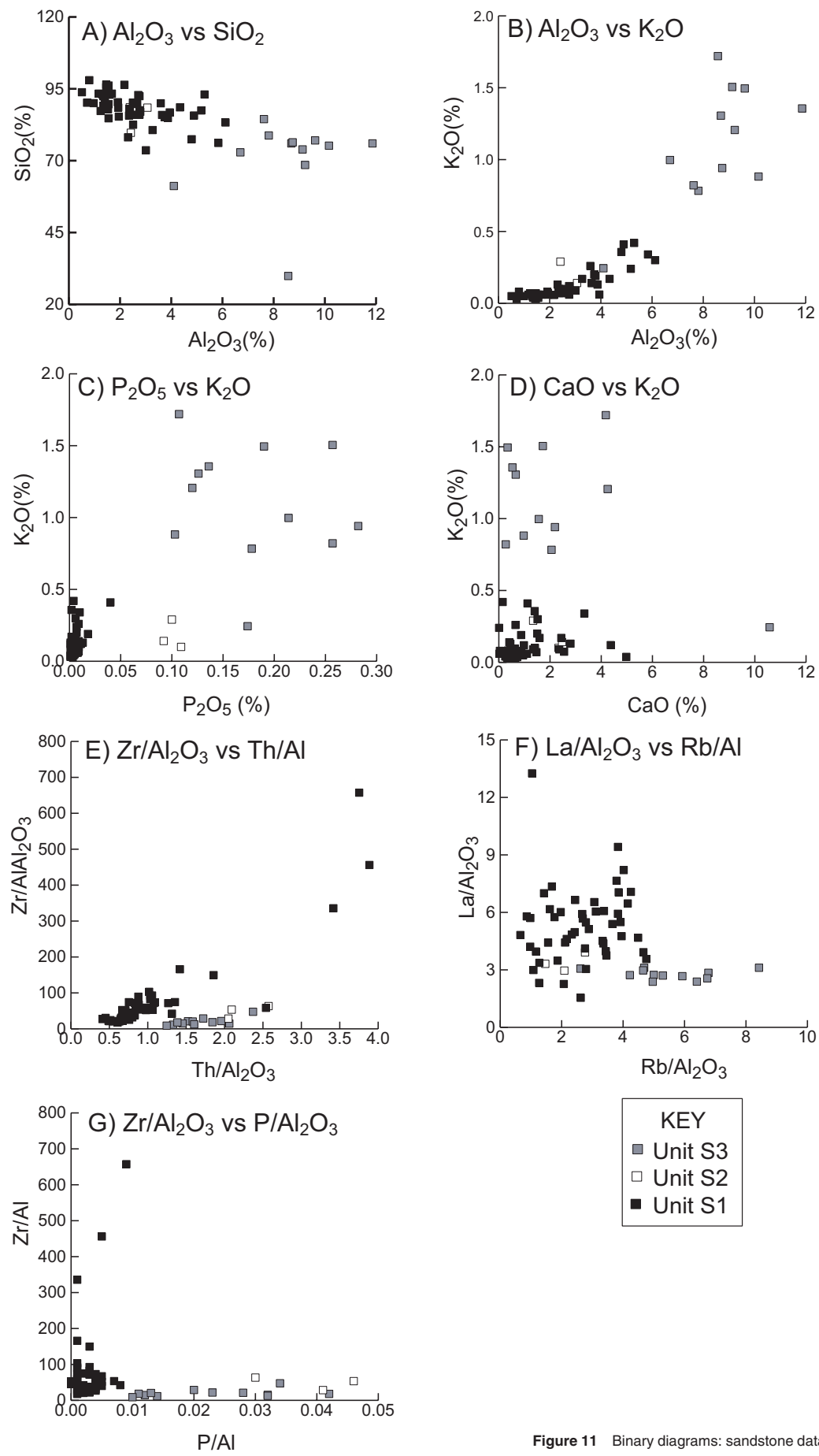


Figure 11 Binary diagrams: sandstone data from wells 44/21-3 and 44/21-7.

Carboniferous sequences and their onshore equivalents in the English Midlands were probably deposited in broadly similar environments and under the same overall climatic conditions. The Etruria Formation (Duckmantian–Bolsovian) contains ferruginous palaeosols and kaolinite is the predominant clay mineral (Besly et al. 1993). However, caliches occur in the overlying Halesowen and Salop formations of Westphalian to early Stephanian age (Besly & Cleal 1997); illite/mica is the main clay mineral, along with minor chlorite (Besly et al. 1993). Similar features are recognized in the equivalent offshore sequences. The aforesaid mineralogical differences indicate climate change, in that the Etruria Formation (= Lower Ketch Unit) was deposited under humid conditions, whereas the Halesowen and Salop formations (= Upper Ketch unit) accumulated in a drier, more arid environment (Besly 1987, Besly et al. 1993). Caliches also occur in overbank sediments of Westphalian D and younger ages in the eastern Netherlands and northern Germany (Besly et al. 1993, Pagnier & van Tongeren 1996). This evidence all shows that climate changed during Westphalian D times. Comparable climate-controlled changes in facies have also been recognized in early Westphalian D successions from the Appalachian Basin (Cecil et al. 1985).

In well 44/21-3, grey coaly intercalations from what is equivalent to the basal part of S3b have yielded a "... late Westphalian C palynoflora (upper part of SL zone)" (Besly et al. 1993: 729). However, new palynological data (Pearce et al. 2005) now assigns a Westphalian D age to this interval, which is broadly comparable with the age of the base of the Halesowen Formation (Besly & Cleal 1997). The different clay mineral assemblages of the Lower and Upper Ketch units, as interpreted from their mudstone geochemistry, and the presence of caliches in the Upper Ketch unit, which indicates climate change, have been confirmed by mineralogical data acquired for the well 44/21-3 chemostratigraphical study (Pearce et al. 2005).

The sedimentology of the Schooner Formation also reflects climate change. The thick sandstone-rich intervals corresponding to S1d–f were deposited on an alluvial fan, with common ferruginous palaeosols and kaolinitic mudstones indicating intense chemical weathering in a humid climate. Geochemical palaeopedology parameters (alumina/bases ratio –  $Al_2O_3/(CaO+MgO+Na_2O+K_2O)$  of Retallack 1997) confirm this and show that the S1 mudstones have suffered relatively severe hydrolytic weathering (Pearce et al. 2005). Rainfall rates then dropped during the deposition of units S2 and S3 (latest Bolsovian to Westphalian D time). Lower-energy floodplain sedimentation prevailed, with sandstones being sporadically deposited in fluvial channels and minor lacustrine deltas, along with the establishment of mature palaeosols and caliches. Furthermore, detrital clay minerals were preserved in the mudstones, although local fluctuations in the water table allowed occasional grey mudstones and thin coals to be retained (Besly 2002, Pearce et al. 2005). The highest values for the alumina/bases ratios are recorded at the top of S1 and at the S2a/S2b boundary, so they may signify breaks in deposition. The S1c mudstones have slightly higher  $Al_2O_3/(CaO+MgO+Na_2O+K_2O)$  values than the S1b and S1d mudstones, reflecting increased pedogenic leaching caused by a probable change in basin topography or water-table conditions (Retallack 1997, Pearce et al. 2005).

## 6.2 Geochemistry and provenance

Clear differences in geochemistry have been used to highlight variations in mineralogical characteristics between the sandstones from S1 and S2 and those from S3. These stratigraphical changes in sandstone mineralogy have a major impact on exploration. The S3 sandstones have poorer reservoir quality than the thicker, porous sandstones from the upper part of S1, so further successful exploration may depend on determining whether Schooner Formation sandstones have either S3 or S1/S2 geochemical signatures.

The differences in sandstone composition can be recognized from the point-count data, heavy-mineral data (Pearce et al. 2005) and the geochemical data, with the two compositional types being interbedded in S2. Besly (1995) attributed such differences to a change in provenance and believed that the Etruria Formation is the onshore equivalent of the Lower Ketch Unit, noting that the composition of the Upper Ketch sandstones is identical to those of the Halesowen Formation. The source for the S1 sandstones is probably the high-grade metamorphic complexes of the Ringkøbing–Fyn High (Morton et al. 2005). Moreover, isotopic data for the Lower Ketch Unit from well 44/21-3 suggest a provenance age of c. 1148Ma–1268Ma (Pearce et al. 2005), which is consistent with derivation from such northeasterly sources as southern Norway and the Oslo Rift.

## 7. Chemostratigraphical correlation

An extensive geochemical dataset has been acquired from the Upper Carboniferous successions encountered in more than 40 wells from UK Quadrants 44 and 49 (Fig. 1) and from Dutch quadrants D, E and F. Much of these data come from cuttings. Only major long-term changes in sediment geochemistry (i.e. those related to provenance or climate changes) can be recognized from cuttings data, although these changes can usually be recognized across an individual field and can even persist sub-regionally. Indeed, when considering stratigraphical trends in sediment geochemistry over thick sequences such as the Schooner Formation, even the distributions of potentially mobile elements such as  $K_2O$ , Rb, Cs and the REEs can form the basis for broad subregional chemostratigraphical correlations. Units S2 and S3 can be recognized and correlated over a wide area, as can sub-units S1a,b and sub-units S1c–S1f, but the correlation of the individual sub-units is usually possible only over an individual field.

Changes in the clay-mineral assemblages of units S2 and S3, and certain of their sedimentological characteristics, reflect a change in climate, with those interpreted changes in mineralogy and depositional environment at the base of S2 being regarded as a subregional "marker". Moreover, the different provenance of the Upper Ketch Unit provides an additional foundation for a chemostratigraphical correlation. However, this provenance change will probably be diachronous across the southern North Sea, because of the northeastward progradation of the fluvial system that deposited S3.

The geochemistry and mineralogy of the Schooner Formation in well 44/21-3 are broadly comparable to that of the onshore Upper Carboniferous sequences in the English Midlands (Pearce et al. 1999), whereas the lithic clast types found in the Bolsovian–Westphalian D sandstones from Quadrants 52

CHEMOSTRATIGRAPHY OF THE UPPER CARBONIFEROUS SCHOONER FORMATION

and 53 and from Lincolnshire (Collinson et al. 1993) suggest comparison with the Upper Ketch unit. Unit S1 broadly correlates with the Etruria Formation (Besly & Cleal 1997, Pearce et al. 1999). They both accumulated at the same time, in similar depositional environments and under similar climatic conditions, but the sandstones of each succession had different source areas being derived mainly from the west in the onshore West Midlands and from the northeast in the southern North Sea (Besly 2002, Morton et al. 2005, Pearce et al. 2005). In geochemical terms, the Halesowen and Salop formations are equivalent to S3 and both were sourced from the Variscan front. Although they have similar "provenance signatures", the Halesowen Formation and S3 were probably derived from different parts of the front, as they have slightly different heavy-mineral assemblages and Sm-Nd isotopic signatures (Pearce et al. 2005). The Halesowen Formation rests unconformably on the Etruria Formation, but sedimentation appears to have been continuous in the southern North Sea.

Red laminated mudstone beds of the Permian Silverpit Formation overlie the Schooner Formation in well 44/21-3, with the base of the Permian (= Saalian unconformity) being at 12 558 ft (Cameron 1993). The Silverpit Formation is equivalent to unit P. Only one analyzed sample (12 552.5 ft) is assigned to this unit, which has similar geochemical characteristics to those of S3b and S3c, apart from a much higher K<sub>2</sub>O level, because of abundant illite/mica. The sample also has a high Na<sub>2</sub>O level, because evaporite minerals are common in the Silverpit Formation. The geochemical similarity between units P and S3 is probably attributable to some S3 material being reworked during a period of erosion associated with the Saalian unconformity.

The base of S1 in well 44/21-3 is defined by a downhole

reduction in Fe<sub>2</sub>O<sub>3</sub>, Cr and Nb contents, along with lower Fe<sub>2</sub>O<sub>3</sub>/MgO, TiO<sub>2</sub>/K<sub>2</sub>O, Nb/Rb, Cr/Cs, and Ta/U ratio values (Figs 3–5). Unit W below has relatively higher MgO, Na<sub>2</sub>O and Cs/La ratio values (Figs 3–5), but, even so, its overall geochemistry is only very slightly different from that of the basal part of S1. In wells to the north, however, the geochemical differences between the Schooner Formation and the Westoe Coal Formation are more marked, because sub-units S1c to S1f overlie the coaly successions.

The base of the Schooner Formation can be recognized using palynology. Strata associated with S1a yield a diagnostic assemblage of reworked late Dinantian to Namurian palynomorphs. Similar reworked assemblages occur at the base of the Schooner Formation in many well sections in Quadrants 44 and 49 (McLean et al. 2005). Furthermore, in well 44/21-3 palynological data indicate that S1a (= Biozone W6b of Late Bolsovian age) lies directly on Biozone W5b of early Bolsovian age (Pearce et al. 2005) confirming the present of an unconformity at the base of the Schooner Formation (McLean et al. 2005). The Schooner Formation overlies the Bolsovian Westoe Coal Formation in well 44/21-3, whereas in wells to the northeast, the formation progressively onlaps Duckmantian, Langsettian and Namurian sequences, where the absence of several biozones across the unconformity makes the base of the formation very obvious.

7.1 Chemostratigraphical correlation of wells 44/21-3 and 44/26c-6

Well 44/21-3 is in the Boulton field and lies about 30 km north of well 44/26c-6 (see Fig. 1). Figure 12 presents the chemostratigraphical correlation of the Schooner Formation between both

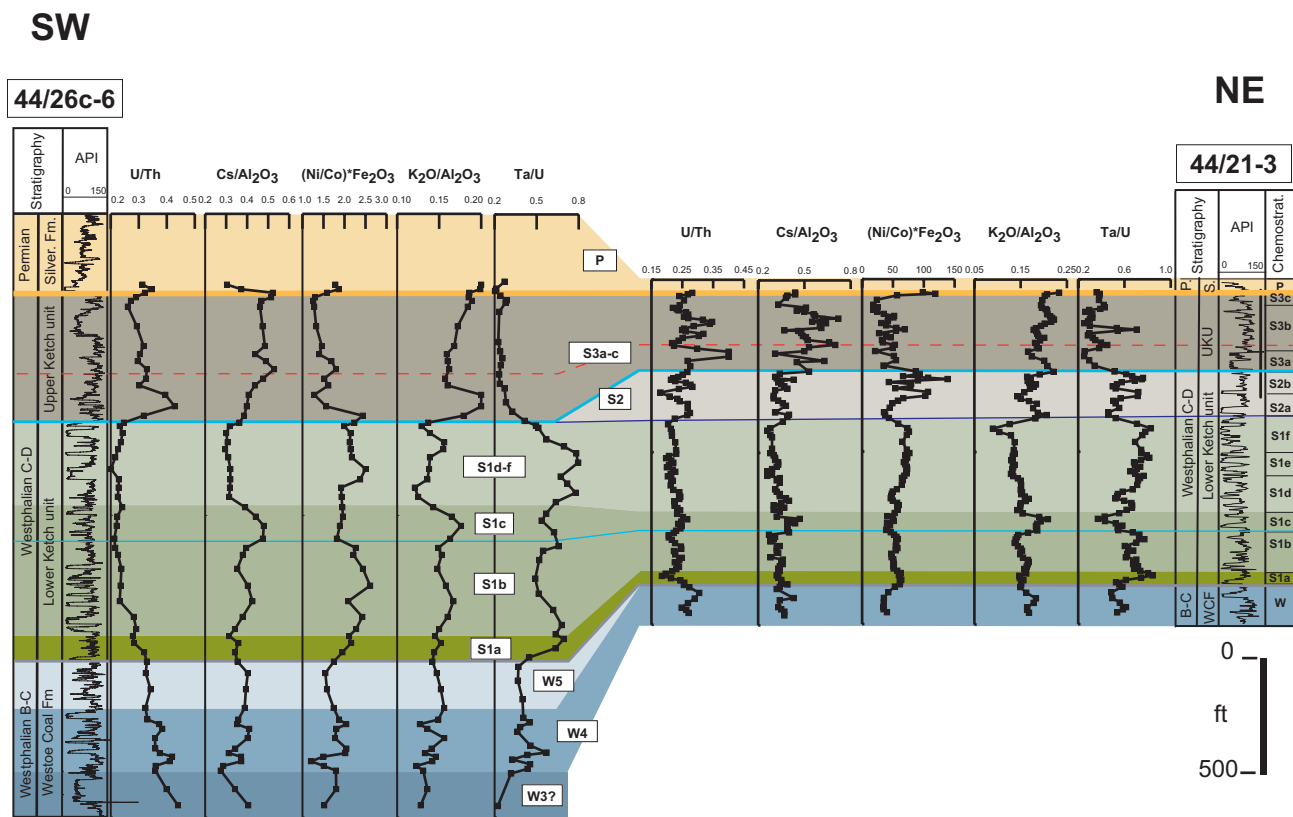


Figure 12 Chemostratigraphical correlation of wells 44/21-3 and 44/26c-6.

T. J. PEARCE, D. WRAY, K. RATCLIFFE, D. K. WRIGHT, A. MOSCARIELLO

wells and illustrates the geochemical parameters on which the correlation is based. The figure also shows that the overall geochemical signature of the formation remains consistent subregionally, and demonstrates how marked steps on the geochemical profiles are used to place the Saalian unconformity and the boundary between the Schooner Formation and the Westoe Coal Formation.

Significant geochemical changes define the top of S1f (= top of S1) in both wells, with the high  $K_2O$ , Rb and Cs ratio values that characterize S1c in well 44/21-3 likewise being recognized in well 44/26c-6. This sub-unit is not so clearly defined in the latter well, though, because of its smaller dataset. Important geochemical differences are also recognized between the two wells; for instance, the moderately high Ta/U values, low Cs/ $Al_2O_3$  values and low U/Th ratios that characterize S2 in well 44/21-3 are not recorded from well 44/26c-6. Accordingly, the base of S3 in well 44/26c-6 may be an unconformity, with the S2 section being lost through erosion. Unit S2 is present in wells to the north, although, here too, the base of S3 is unconformable. The deposition of S3 marks the influx of sediments derived from the southern Variscan source area, which supplied detritus to the area throughout Westphalian D times. Units S1 and S2 are genetically linked, as the corresponding sediments of both units have a similar northern Caledonian provenance, even though the mineral and geochemical characteristics of the S2 mudstones provide evidence for an increasingly arid climate.

### 8. The use of chemostratigraphy

Significant failings were found in the reservoir zonation of the Schooner field (Block 44/26) once production was initiated (Stone & Moscariello 1999), the zonation being based mainly on wireline log data (Fig. 13a). As pressure-data measurements did not confirm the proposed reservoir connectivity model, the original zonation seems to be flawed. To help with this problem, chemostratigraphy has been applied to wells in the Schooner field, with the establishment of a five-fold chemostratigraphical zonation by Chemostrat Ltd (Fig. 13b). Moscariello (2000) also undertook a detailed pedofacies study of the successions, employing sonic data and facies data from core to enhance the chemostratigraphical zonation (Moscariello 2003). Consequently, a new reservoir model for the Schooner field has been proposed, which in turn has led to a new depositional model for the Schooner Formation. Extensive lateral connectivity of the unit 1 and 2 sandstones is found in the west of the field, before the main sandstone fairway switched to the east during the deposition of units 4 and 5. This new zonation seems valid, as the predicted pressure depletion model appears to coincide closely with actual pressure readings measured during production (Fig. 14), in contrast to the old reservoir model.

Chemostratigraphy is being used in the Hawksley field (Block 44/17) to confirm the stratigraphy of bottom hole sections where the wells have encountered the Schooner Formation (Conway et al. 2002). All the S1 sequences need to be penetrated, so as to ensure that all the potential gas reservoirs have been drilled. Furthermore, chemostratigraphy confirms the depth of the Saalian unconformity and the lithostratigraphy of those sequences assigned to units S2 and S3.

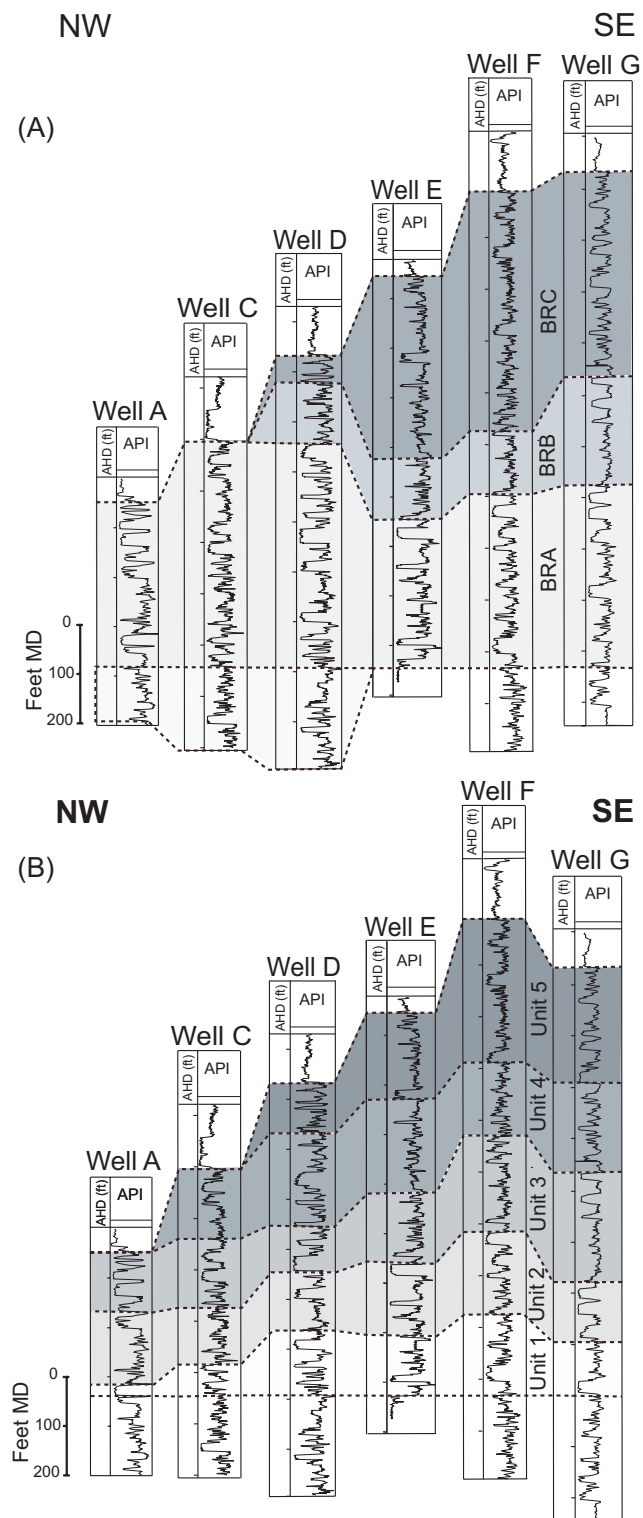


**Figure 13** Reservoir zonation for the Schooner Formation, Schooner field (modified from Stone & Moscariello 1999). (a) Original correlation datum = base of the Barren Red Measures (= Schooner Formation), showing zones A, B and C. (b) Chemostratigraphical correlation, showing units 1 to 5.

### 9. Summary and conclusions

In UK Quadrants 44 and 49, well sections through the hydrocarbon-bearing Upper Carboniferous Schooner Formation (Barren Red Measures) are difficult to correlate by established methods, as they yield little reliable biostratigraphical data, and wireline

## CHEMOSTRATIGRAPHY OF THE UPPER CARBONIFEROUS SCHOONER FORMATION

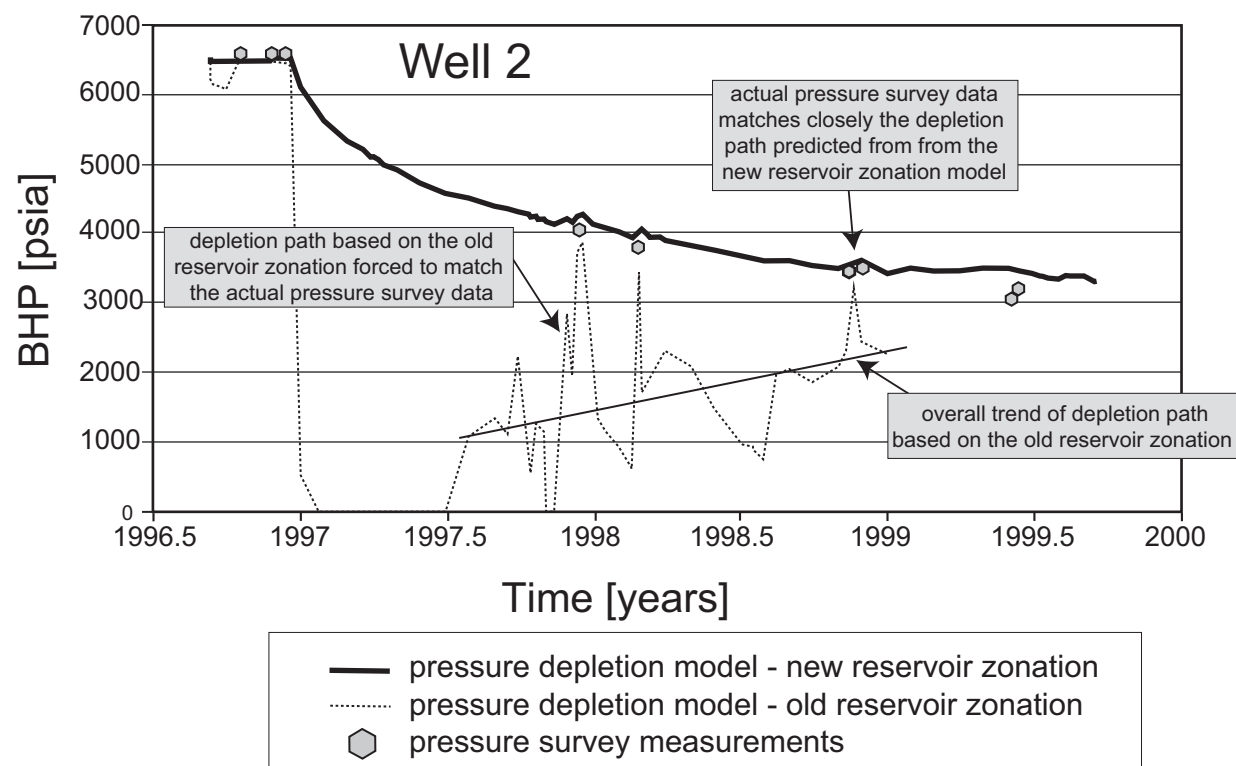


**Figure 14** Pressure depletion of the entire reservoir for one well through the Schooner field (modified from Moscariello 2003). The graphs illustrate the depletion of the reservoir based on the original lithostratigraphical zonation and how it was forced to match the actual pressure measurements. Also illustrated is the predicted depletion pathway for the reservoir based on the chemostratigraphical zonation, which closely matches the actual measurements.

log traces are not particularly distinctive. Chemostratigraphy has been applied to these sections to improve their interwell correlation.

Chemostratigraphy is based on the recognition of stratigraphical variations in the inorganic geochemistry of the sedimentary sequences, although the success of the technique depends on relating geochemical variations to changes in mineralogy. Such changes are, in turn, controlled by provenance, depositional processes and environments, weathering and diagenesis. One important advantage of chemostratigraphy is that ICP analyses can acquire reliable geochemical data from core samples and cuttings, only small sample volumes being required.

The study centres on well 44/21-3, which has penetrated one of the most complete Schooner Formation successions in the Silverpit Basin. The formation is divided into S1 (= the Lower Schooner Unit and most of the Lower Ketch Unit), S2 (= uppermost part of the Lower Ketch Unit) and S3 (= Upper Ketch Unit), with these units themselves being divided into chemostratigraphical sub-units on the basis of subtle geochemical variations. The study also demonstrates the base of the Schooner Formation corresponds to a subregional unconformity.

The chemostratigraphical units are defined by using the mudstone data and sandstone data, and the differentiation of the units ultimately can be related to changes in provenance and climate. The S1 mudstones have high levels of  $Al_2O_3$ ,  $Fe_2O_3$ , LREES and  $TiO_2$ , which reflect the abundance of kaolinite, Fe- and Al-oxyhydroxides and anatase. In contrast, the S3 mudstones have high levels of  $K_2O$ , Rb and Cs, because illite/mica is more abundant in these mudstones. A few S3 mudstone samples also have high CaO, MgO and MnO contents, these samples coming from caliches and argillaceous lacustrine limestones. The S2 mudstones have intermediate  $K_2O$ , Rb, Cs and  $Al_2O_3$  contents. Similar

geochemical and mineralogical characteristics are found in the Upper Carboniferous mudstones of central England and elsewhere in the southern North Sea. Consequently, these stratigraphical changes in mudstone geochemistry reflect a progressive change from humid conditions to more arid climates during the deposition of the S2 and S3 sequences, rather than just localized facies changes.

An important provenance change recognized from the Upper Carboniferous sandstones in central England can also be identified in well 44/21-3. Unit S1 sandstones have very high  $SiO_2$  levels and relatively high  $TiO_2$ , Nb, Ta and Zr levels, which show that they are quartzitic and have zircon-rutile-tourmaline heavy-mineral assemblages. These geochemical and mineralogical characteristics indicate that the sandstones have been derived from a high-grade metamorphic terrain, probably situated in southern Norway. In contrast, a few S2 sandstones and all the S3 sandstones have higher  $K_2O$ , CaO,  $Na_2O$ , Rb and Cs levels, and higher Th/Zr and  $P_2O_5/Zr$  values, which show these sandstones contain quartz, feldspar, mica and schistose and phyllitic clasts; their heavy-mineral assemblages consist of abundant apatite, traces of garnet and less zircon than in the S1 sandstones. The bulk mineralogy and geochemistry of S3 are similar to the onshore "Pennant facies". Both are diachronous and prograded northwards as sediment was sourced from the mountain ranges associated with the uplifted Variscan front (Besly 2002).

The important geochemical characteristics of the well 44/21-3 study interval are also recognized in other well sections through the Schooner Formation, thus enabling a subregional interwell chemostratigraphical correlation to be erected. The viability of the correlation is corroborated by the new biostratigraphical data (McLean et al. 2005, Pearce et al. 2005). The

T. J. PEARCE, D. WRAY, K. RATCLIFFE, D. K. WRIGHT, A. MOSCARIELLO

resolution of the interwell correlation is particularly good on the scale of an individual field, where the defining geochemical features of the correlation reflect subtle changes in detrital mineralogy and facies. On the subregional scale, only the chemostratigraphical units can be correlated, this correlation being based on geochemical characteristics governed by changes in provenance and climate.

Chemostratigraphy can produce the foundation for a reliable stratigraphical framework. Proprietary chemostratigraphical studies on the Schooner Formation and its equivalents in Quadrants 44 and 49 and from Dutch sector Quadrants D, E and F have recognized similar chemostratigraphical units and sub-units to those in well 44/21-3, so allowing interwell chemostratigraphical correlations to be erected for this formation across much of the southern North Sea. However, chemostratigraphy produces the best results when it is part of a multidisciplinary study (Pearce et al. 2005).

### Acknowledgements

The authors wish to thank Conoco UK Ltd and Shell UK Exploration and Production Ltd, plus their respective partners, for access to samples and for permission to publish the paper. In addition, the work of Lorna Dyer from the Department of Earth Sciences, University of Greenwich, is greatly appreciated. Constructive reviews of this manuscript by two reviewers are gratefully acknowledged, although the views expressed in this paper are those of the authors alone.

### References

- Andrew, A. S., D. J. Whitford, P. J. Hamilton, S. Scarano, M. Buckley 1996. Application of chemostratigraphy to petroleum exploration and field appraisal: an example from the Surat Basin. Paper (37008) presented at the SPE Asia Pacific Oil & Gas conference, Adelaide, October 1996, 421–9.
- Bailey, J. B., P. Arbin, O. Daffinoti, P. Gibson, J. S. Ritchie 1993. Permo-Carboniferous plays of the Silver Pit Basin. In *Petroleum geology of northwest Europe: proceedings of the 4th conference*, J. R. Parker (ed.), 707–715. London: Geological Society.
- Besly, B. M. 1987. Sedimentological evidence for Carboniferous and Early Permian palaeoclimates of Europe. *Societe géologique du Nord, Annales* **106**, 131–43.
- 1995. Stratigraphy of Late Carboniferous redbeds in the southern North Sea and adjoining land areas. Paper presented at “Stratigraphic advances in the offshore Devonian and Carboniferous rocks, UKCS and adjacent onshore areas” conference, Geological Society, London, January 1995.
- 2002. Late Carboniferous redbeds of the UK southern North Sea viewed in a regional context [abstract: pp. 17–20]. This volume: 225–226.
- Besly, B. M. & C. J. Cleal 1997. Upper Carboniferous stratigraphy of the West Midlands (UK) revised in the light of borehole geophysical logs and detrital compositional suites. *Geological Journal* **32**, 85–118.
- Besly, B. M., S. D. Burley, P. Turner 1993. The late Carboniferous “Barren Red Bed” play of the Silver Pit area, southern North Sea. In *Petroleum geology of northwest Europe: proceedings of the 4th conference*, J. R. Parker (ed.), 727–40. London: Geological Society.
- Blatt, H., G. Middleton, R. Murray 1972. *Origin of sedimentary rocks*. Englewood Cliffs, New Jersey: Prentice-Hall.
- Cameron, T. D. J. 1993. Carboniferous and Devonian of the southern North Sea. In *Lithostratigraphic nomenclature of the UK North Sea* (vol. 5), R. W. O’B. Knox & W. G. Cordey (eds), 1–93. Nottingham: British Geological Survey.
- Cameron, T. D. J., A. Crosby, P. S. Balson, D. H. Jeffrey, G. K. Lott, J. Bulat, D. J. Harrison 1992. *The geology of the southern North Sea*. United Kingdom Offshore Regional Report, British Geological Survey, Keyworth, Nottingham.
- Cecil, C. B., R. W. Stanton, S. G. Neuzil, R. T. Dulong, L. F. Ruppert, B. S. Pierce 1985. Paleoclimate controls on Late Paleozoic sedimentation and peat formation in the Central Appalachian Basin. *International Journal of Coal Geology* **5**, 195–230.
- Collinson, J. D., C. M. Jones, G. A. Blackbourn, B. M. Besly, G. M. Archard, A. H. McMahon 1993. Carboniferous depositional systems of the southern North Sea. In *Petroleum geology of northwest Europe: proceedings of the 4th conference*, J. R. Parker (ed.), 677–87. London: Geological Society.
- Conway, A. M., I. M. Fozdar, R. Ings 2002. CMS III realizing a cluster development of Westphalian B and C/D reservoirs [abstract: p. 23]. Paper presented at “Hydrocarbon resources of the Carboniferous, southern North Sea and surrounding areas” conference, Yorkshire Geological Society, Sheffield, September 2002.
- Cullers, R. L. 1995. The controls on the major- and trace-element evolution of shales, siltstones and sandstones of Ordovician to Tertiary age in the West Mountains region, Colorado, USA. *Chemical Geology* **123**, 107–131.
- Ehrenberg, S. N. & E. Siring 1992. Use of bulk chemical analysis in stratigraphic correlation of sandstones: an example from the Statfjord Nord field, Norwegian continental shelf. *Journal of Sedimentary Petrology* **62**, 318–30.
- Hauger, E., R. Lovlie, P. Van Veen 1994. Magnetostratigraphy of the Middle Jurassic Brent Group in the Oseberg oil field, northern North Sea. *Marine and Petroleum Geology* **11**, 375–88.
- Herron, M. M. 1988. Geochemical classification of terrigenous sediments using log or core data. *Journal of Sedimentary Petrology* **58**, 820–29.
- Jarvis, I. & K. E. Jarvis 1992a. Inductively coupled plasma-atomic emission spectrometry in exploration geochemistry. In *Analytical methods in geochemical exploration*, G. E. M. Hall & B. Vaughlin (eds), 139–200. *Journal of Geochemical Exploration*, special issue 44.
- 1992b. Plasma spectrometry in earth sciences: techniques, applications and future trends. In *Plasma spectrometry in Earth sciences*, I. Jarvis & K. E. Jarvis (eds), 1–33. *Chemical Geology* **95**, special issue.
- Kramer, W., G. R. Weatherall, R. Offler 2001. Origin and correlation of tuffs in the Permian Newcastle and Wollombi Coal Measures, NSW, Australia, using chemical fingerprinting. *International Journal of Coal Geology* **47**, 115–35.
- Leeder, M. R. & M. Hardman 1990. Carboniferous geology of the Southern North Sea Basin and controls on hydrocarbon prospectivity. In *Tectonic events responsible for Britain’s oil and gas reserves*, R. F. P. Hardman & J. Brooks (eds), 87–105. Special Publication 55, Geological Society, London.
- Mange-Rajetzky, M. A. 1995. Subdivision and correlation of monotonous sandstone sequences using high-resolution heavy-mineral analysis, a case study: the Triassic of the Central Graben. In *Non-biostratigraphical methods of dating and correlation*, R. E. Dunay & E. A. Hailwood (eds), 23–30. Special Publication 89, Geological Society, London.
- McBride, E. F. 1963. A classification of common sandstones. *Journal of Sedimentary Petrology* **33**, 664–9.
- McLean, D., B. Owens, R. Neves 2005. Carboniferous miospore biostratigraphy of the North Sea. This volume: 13–24.
- Mearns, E. W. 1988. A samarium–neodymium isotope survey of modern river sediments from northern Britain. *Chemical Geology* **73**, 1–13.
- 1989. Neodymium isotope stratigraphy of Gullfaks oil field. In *Correlation in hydrocarbon exploration*, J. D. Collinson (ed), 201–15. London: Graham & Trotman.
- Morton, A. C. 1985. Heavy minerals in provenance studies. In *Provenance of arenites*, G. G. Zuffa (ed.), 249–77. Dordrecht: Reidel.
- 1991. Geochemical studies of detrital heavy minerals and their application to provenance studies. In *Developments in sedimentary provenance studies*, A. C. Morton, S. P. Todd, P. D. W. Haughton

## CHEMOSTRATIGRAPHY OF THE UPPER CARBONIFEROUS SCHOONER FORMATION

- (eds), 31–45. Special Publication 57, Geology Society, London.
- Morton, A. C. & C. Hallsworth 1994. Identifying provenance-specific features of detrital heavy-mineral assemblages in sandstones. *Sedimentary Geology* **90**, 241–56.
- Morton, A. C. & A. Hurst 1995. Correlation of sandstones using heavy minerals: an example from the Staffjord Formation of the Snorre field, northern North Sea. In *Non-biostratigraphical methods of dating and correlation*, R. E. Dunay & E. A. Hailwood (eds), 3–22. Special Publication 89, Geology Society, London.
- Morton, A. C., C. Hallsworth, A. Moscariello 2005. Interplay between northern and southern sediment sources during Westphalian deposition in the Silverpit Basin, southern North Sea. This volume: 135–146.
- Moscariello, A. 2000. Pedofacies in reservoir modelling of low net to gross, barren fluvial sequences (Schooner Formation, Carboniferous SNS). EAGE 62nd Conference and Technical Exhibition, 1–4.
- 2003. The Schooner field, blocks 44/26a and 43/30a, UK southern North Sea. In *The United Kingdom oil and gas fields commemorative millennium volume*, J. Gluyas & H. Hichens (eds), 811–24. Memoir 20, Geological Society, London.
- Pagnier, H. J. M. & P. C. H. van Tongeren 1996. Upper Carboniferous of borehole “De Lutte-6” and evaluation of the Tubbergen Formation in the eastern and southeastern parts of the Netherlands. *Mededelingen Rijks Geologische Dienst* **55**, 3–30.
- Pearce, T. J. 1991. *The geology, geochemistry, sedimentology and provenance of Late Quaternary turbidites, Madeira Abyssal Plain* PhD thesis, Kingston Polytechnic.
- Pearce, T. J. & I. Jarvis 1992a. The composition and provenance of turbidite sands: Late Quaternary Madeira Abyssal Plain. *Marine Geology* **109**, 21–51.
- 1992b. Applications of geochemical data to modelling sediment dispersal patterns in distal turbidites: Late Quaternary of the Madeira Abyssal Plain. *Journal of Sedimentary Petrology* **62**, 1112–29.
- 1995. High-resolution chemostratigraphy of Quaternary distal turbidites: a case study of new methods for the correlation of barren strata. In *Dating and correlating biostratigraphically barren strata*, R. E. Dunay & E. A. Hailwood (eds), 107–43. Special Publication 89, Geology Society, London.
- Pearce, T. J., B. M. Besly, D. Wray, D. K. Wright 1999. Chemostratigraphy: a method to improve interwell correlation in barren sequences – a case study using Duckmantian/Stephanian sequences (West Midlands, UK). *Sedimentary Geology* **124**, 197–220.
- Pearce, T. J., D. McLean, D. K. Wright, C. J. Jeans, E. W. Mearns 2005. Stratigraphy of the Upper Carboniferous Schooner Formation, southern North Sea: chemostratigraphy, mineralogy, palynology and Sm–Nd isotope analysis. This volume: 165–182.
- Pettijohn, F. J. 1975. *Sedimentary rocks*, 3rd edn. New York: Harper Row.
- Preston, J., A. Hartley, M. Hole, S. Buck, J. Bond, M. Mange, J. Still 1998. Integrated whole-rock trace-element geochemistry and heavy-mineral chemistry studies: aids to the correlation of continental redbed reservoirs in the Beryl field, UK North Sea. *Petroleum Geoscience* **4**, 7–16.
- Racey, A., M. A. Love, R. M. Bobolecki, J. N. Walsh 1995. The use of chemical element analysis in the study of biostratigraphically barren sequences: an example from the Triassic of the central North Sea (UKCS). In *Non-biostratigraphical methods of dating and correlation*, R. E. Dunay & E. A. Hailwood (eds), 69–105. Special Publication 89, Geology Society, London.
- Ratcliffe, K. T., T. J. Pearce, J. Martin, A. D. Hughes, in press. Enhanced reservoir characterization of the Triassic Argilo Gresseux-Inferieur, Algeria using high resolution chemostratigraphy. *American Association of Petroleum Geologists, Bulletin* **89**.
- Retallack, G. J. 1997. *A colour guide to palaeosols*. Chichester, England: John Wiley.
- Scholle, P. A. 1979. *A color illustrated guide to constituent textures, cements and porosities of sandstones and associated rocks*. Memoir 28, American Association of Petroleum Geologists, Tulsa, Oklahoma.
- Shail, R. D. & P. A. Floyd 1988. An evaluation of flysch provenance – example from the Gramscatho Group of southern Cornwall. *Ussher Society, Proceedings* **7**, 62–6.
- Spears, D. A. & M. A. Amin 1981. A mineralogical and geochemical study of turbidite sandstones and interbedded shales, Mam Tor, Derbyshire, UK. *Clay Minerals* **16**, 333–45.
- Stone, G. & A. Moscariello 1999. Integrated modelling of the southern North Sea Carboniferous Barren Red Measures using production data, geochemistry, and pedofacies cyclicity. Paper (56898) presented at the SPE Offshore Europe 99 conference, Aberdeen, September 1999, 1–8.

